Published in final edited form as:
J Comp Neurol. 2009 January 1; 512(1): 6–26. doi:10.1002/cne.21846.

Plasmalemmal and Vesicular γ-Aminobutyric Acid Transporter Expression in the Developing Mouse Retina

CHENYING GUO[1], **SALVATORE L. STELLA JR.**[1], **ARLENE A. HIRANO**[1], and **NICHOLAS C. BRECHA**[1,2,3,4,5,*]

[1]Department of Neurobiology, David Geffen School of Medicine at UCLA, University of California, Los Angeles, California 90095

[2]Department of Medicine, David Geffen School of Medicine at UCLA, University of California, Los Angeles, California 90095

[3]Jules Stein Eye Institute, David Geffen School of Medicine at UCLA, University of California, Los Angeles, California 90095

[4]CURE-Digestive Diseases Research Center, David Geffen School of Medicine at UCLA, University of California, Los Angeles, California 90095

[5]Veterans Administration Greater Los Angeles Healthcare System, Los Angeles, California 90073

Abstract

Plasmalemmal and vesicular γ-aminobutyric acid (GABA) transporters influence neurotransmission by regulating high-affinity GABA uptake and GABA release into the synaptic cleft and extracellular space. Postnatal expression of the plasmalemmal GABA transporter-1 (GAT-1), GAT-3, and the vesicular GABA/glycine transporter (VGAT) were evaluated in the developing mouse retina by using immunohistochemistry with affinity-purified antibodies. Weak transporter immunoreactivity was observed in the inner retina at postnatal day 0 (P0). GAT-1 immunostaining at P0 and at older ages was in amacrine and displaced amacrine cells in the inner nuclear layer (INL) and ganglion cell layer (GCL), respectively, and in their processes in the inner plexiform layer (IPL). At P10, weak GAT-1 immunostaining was in Müller cell processes. GAT-3 immunostaining at P0 and older ages was in amacrine cells and their processes, as well as in Müller cells and their processes that extended radially across the retina. At P10, Müller cell somata were observed in the middle of the INL. VGAT immunostaining was present at P0 and older ages in amacrine cells in the INL as well as processes in the IPL. At P5, weak VGAT immunostaining was also observed in horizontal cell somata and processes. By P15, the GAT and VGAT immunostaining patterns appear similar to the adult immunostaining patterns; they reached adult levels by about P20. These findings demonstrate that GABA uptake and release are initially established in the inner retina during the first postnatal week and that these systems subsequently mature in the outer retina during the second postnatal week.

Keywords

GAT; VGAT; amacrine cells; horizontal cells; retina; visual system

Plasmalemmal and vesicular γ-aminobutyric acid (GABA) transporters have essential roles in GABA neurotransmission. The GABA plasma membrane transporters (GATs), which mediate high-affinity GABA uptake from the synaptic cleft and extracellular space, terminate GABA's

*Correspondence to: Nicholas C. Brecha, PhD, Department of Neurobiology, David Geffen School of Medicine at UCLA, University of California at Los Angeles, 10833 Le Conte Ave., Los Angeles, CA 90095-1763. E-mail: nbrecha@ucla.edu.

synaptic action (for reviews see Chen et al., 2004; Conti et al., 2004; Kanner, 2006). In addition, GATs have been proposed to mediate GABA release into the extracellular space in both normal and pathological conditions (Schwartz, 1987, 2002; O'Malley et al., 1992; Attwell et al., 1993; Dalby, 2003; Richerson and Wu, 2003; Wu et al., 2007). The vesicular GABA transporter (VGAT or VIAAT) mediates GABA uptake and storage in synaptic vesicles (for review see Gasnier, 2004) before GABA is released from synaptic vesicles by a Ca^{2+}-dependent mechanism following depolarization of the nerve terminal (Liu and Edwards, 1997; Südhof, 2004).

Four distinct molecular and pharmacological types of GATs, GAT-1, GAT-2, GAT-3, and betaine/GABA transporter (BGT-1),[1] have been identified in the mammalian nervous system (for reviews see Nelson, 1998; Conti et al., 2004). GAT-1, -2, and -3 are high-affinity GABA transporters, whereas BGT-1 is a low-affinity GABA transporter (Nelson, 1998; Chen et al., 2004). These plasma membrane transporters are members of the Na^+- and Cl^--dependent transporter family, solute carrier family (SLC) 6. They share a common structural topology of 12 putative transmembrane spanning segments, and they have a 50 -70% identity in their predicted amino acid sequences (Kanner, 2006).[1] These plasma membrane transporters have different pharmacological properties, including ionic dependencies and inhibitor sensitivities suggestive of different functional properties (for reviews see Nelson, 1998;Conti et al., 2004; see also Guastella et al., 1990;Borden et al., 1992,1994;Yamauchi et al., 1992;Liu et al., 1993). GAT-1 and GAT-3 have a differential regional distribution in the central nervous system; for instance, in the forebrain, GAT-1 is localized mainly to axonal terminals, and, elsewhere along the neuroaxis, both GAT-1 and GAT-3 are localized to astrocytes (for reviews see Nelson, 1998;Conti et al., 2004; see also Ikegaki et al., 1994;Minelli et al., 1995, 1996;Ribak et al., 1996;De Biasi et al., 1998). GAT-2 is localized mainly to the leptomeninges (Ikegaki et al., 1994;Durkin et al., 1995). GATs mediate GABA transport across the plasma membrane in either direction (Attwell et al., 1993;Lu and Hilgemann, 1999;Richerson and Wu, 2003;Kanner, 2006;Wu et al., 2007). Finally, GAT-1 and GAT-3 are likely to have a strong influence on both phasic and tonic inhibitory neurotransmission, because they mediate high-affinity GABA uptake from the synaptic cleft and extracellular space as well as reverse transport of GABA into the extracellular space (for review see Glykys and Mody, 2007; see also Isaacson et al., 1993;Richerson and Wu, 2003;Keros and Hablitz, 2005;Wu et al., 2007).

In mammalian retina, GAT-1 immunoreactivity is localized mainly to neurons, including amacrine cells and their processes in the inner plexiform layer (IPL; Brecha and Weig-mann, 1994; Honda et al., 1995; Johnson et al., 1996; Hu et al., 1999; Dmitrieva et al., 2001; Casini et al., 2006). In addition, there is a low expression of GAT-1 in Müller cells in rodent retinas (Brecha and Weigmann, 1994; Honda et al., 1995; Johnson et al., 1996; Biedermann et al., 2002). GAT-2 is absent from the retina and is distributed to the retinal pigment and ciliary epithelium (Honda et al., 1995; Johnson et al., 1996). GAT-3 is expressed principally by Müller cells, as well as in amacrine cells, in the mammalian retina (Honda et al., 1995; Johnson et al., 1996; Hu et al., 1999; Biedermann et al., 2002). BGT-1 is a low-affinity GABA transporter and has been localized primarily to glial elements in the CNS (Gadea and López-Colomé, 2001). BGT-1 immunoreactivity has not been reported in the retina. GABA neurotransmission in the retina is influenced by GATs: blocking GAT-1 transport by GAT-1 up-take inhibitors prolongs the decay of $GABA_A$- and $GABA_C$- mediated postsynaptic potentials of bipolar and ganglion cells (Ichinose and Lukasiewicz, 2002; Hull et al., 2006).

[1]The nomenclature of the GAT plasma transporters varies betweenn mice vs. rats, dogs, and humans. The same nomenclature is used to refer to GAT-1, GAT-2, GAT-3, and BGT-1 in rat, dog, and human (Guastella et al., 1990; Borden, 1996; Conti et al., 2004). A different nomenclature is used for mouse (Liu et al., 1993); mouse GAT-1 corresponds to rat and human GAT-1, mouse GAT-2 corresponds to dog and human BGT-1, mouse GAT-3 corresponds to rat GAT-2, and mouse GAT-4 corresponds to rat GAT-3. This paper uses GAT-1 and GAT-3 to refer to mouse GAT-1 and mouse GAT-4, respectively.

The vesicular GABA transporter (VGAT), which is also referred to as the *vesicular inhibitory amino acid transporter* (VIAAT), is the sole member of the SLC32 family with 10 putative transmembrane domains (McIntire et al., 1997; Sagné et al., 1997; Takamori et al., 2000; Gasnier, 2004). VGAT is localized to synaptic vesicles in GABA- and glycine-containing neurons and in some endocrine cells (Chaudhry et al., 1998; Dumoulin et al., 1999; Gammelsaeter et al., 2004). VGAT utilizes a proton electrochemical gradient to mediate GABA and glycine transport into synaptic vesicles (Burger et al., 1991; Christensen et al., 1991; McIntire et al., 1997; Sagné et al., 1997; Takamori et al., 2000). Inhibitory neurotransmission is markedly reduced with deletion of the VGAT gene (Wojcik et al., 2006), highlighting the critical role of this transporter in regulating inhibitory synaptic neurotransmission.

VGAT expression has been reported in the retina of several mammalian species, including mice, rats, and primates (Haverkamp et al., 2000; Cueva et al., 2002; Jellali et al., 2002; Johnson et al., 2003). VGAT immunoreactivity is distributed to both the inner and the outer retina: many amacrine cell somata show weak cytoplasmic VGAT immunostaining, and there is strong VGAT immunoreactivity in amacrine cell processes and terminals in the IPL. VGAT immunoreactivity is also present in all horizontal cell bodies and their processes in the outer plexiform layer (OPL; Haverkamp et al., 2000; Cueva et al., 2002; Jellali et al., 2002).

GABA and its synthetic enzymes, L-glutamate acid decarboxylase-65 (GAD_{65}) and -67 (GAD_{67}), are initially detected in the retina during the late prenatal period, and they are expressed by both amacrine and horizontal cells. In rat retina, GAD activity is detectable at postnatal day 1 (P1), and it increases until it reaches peak activity at P21, before decreasing to adult levels by P30 (Yamasaki et al., 1999). GABA is likewise detectable at P1, and it increases from P8 to adulthood (Yamasaki et al., 1999). Manipulation of GABA signaling is reported to affect outer retinal development, including cone photoreceptor synaptogenesis; furthermore, blockage of ionotropic GABA receptors disrupts the formation of normal cone distribution (Redburn-Johnson, 1998; Huang et al., 2000). Horizontal cells appear to be the source of GABA in the perinatal period in the outer retina, insofar as they contain high levels of GADs and GABA immunoreactivities (Schnitzer and Rusoff, 1984; Osborne et al., 1986). In the inner retina, GABA signaling appears to be established prior to glutamate signaling. For instance, in mouse retina, VGAT is expressed before vesicular glutamate transporters (VGLUT; Johnson et al., 2003). Furthermore, GABAergic spontaneous postsynaptic currents (PSCs) in ganglion cells are first detected at about embryonic day (E17) and presumed glutamatergic PSCs at about P3 (Unsoeld et al., 2008). Spontaneous electrical activity known as *retinal waves*, which occur during early retinal development, is triggered initially by reciprocal nicotinic and GABAergic synapses between starburst amacrine cells. With maturation of the retina, the strength of the nicotinic synapses declines, and the GABAergic synapses convert from excita-tory to inhibitory (Zheng et al., 2004). Together, these findings imply that GABA influences retinal development, including both the synaptic organization and the circuitry formation in the OPL and IPL. Because of the importance of GABA in the development of the retina, we evaluated the expression of both the plasma membrane and the vesicular GABA transporters as they influence GABA levels in the retina.

The aim of the present study was to determine the cellular expression of GAT-1, GAT-3, and VGAT in the developing mouse retina to understand better the functional maturation of these GABA transport systems. Low levels of GAT-1, GAT-3, and VGAT immunoreactivity are present at birth in the inner retina, and the levels increase during the first and second postnatal weeks. GAT-1 is strongly expressed in amacrine cells, and it is weakly expressed in Müller cells during the postnatal period and in the adult retina. In contrast, GAT-3 is strongly expressed in Müller cells as well as some amacrine cells during the postnatal period and in the adult retina. VGAT immunostaining is restricted mainly to amacrine cell bodies and processes in the IPL

and to horizontal cell bodies and processes beginning during the middle to late part of the first postnatal week, in agreement with a previous study (Johnson et al., 2003). These findings suggest that plasmalemmal and vesicular GABA transporter expression is established within the first postnatal week in the inner retina and that transporter expression is subsequently established in the outer retina during the second postnatal week.

MATERIALS AND METHODS

Animals

C57Bl/6J mice (UCLA colony) of either sex were used for these studies. Mice were maintained on a 12-hour light/dark cycle. Mice were killed, and their retinas were collected at postnatal day 0 (P0), P3, P5, P10, P15, P20, P30, and adulthood (ages varied from P48 to 2 years) for the immunostaining studies and from adult retinas (P30–P45) for the Western blot studies. All experiments were performed in accordance with the guidelines for the welfare of experimental animals issued by the UCLA Animal Research Committee, and U.S. Public Health Service Policy on Humane Care and Use of Laboratory Animals. Mice at P0 and P3 were deeply anesthetized via cryoanesthesia and decapitated, and mice at P5 and older were killed with 1–3% isofluorane (Hospira, Inc., Lake Forest, IL). The eyes were enucleated, the cornea and lens were removed, and the eyecups were immersion fixed in 4% (w/v) paraformaldehyde (PFA) in 0.1 M phosphate buffer (PB; pH 7.4) for 30–45 minutes at room temperature. After fixation, the eyes were cryoprotected in 25% sucrose, briefly washed in 0.1 M PB, embedded in OCT compound (Sakura Finetek Inc., Torrance, CA), and rapidly frozen with dry ice. Cryostat sections of the eyecup were cut vertically at 12 μm, mounted on to gelatin-coated slides, air dried, and stored at −20°C.

Antibodies

Primary antibodies were as follows: affinity-purified rabbit polyclonal antibodies directed to the C-terminus of GAT-1 (346O) and GAT-3 [374D; (Johnson et al., 1996)], a rabbit polyclonal antibody against the N-terminus of VGAT (VGAT-N2; Chaudhry et al., 1998), and a mouse monoclonal antibody against VGAT (131 011; Synaptic Systems, Göttingen, Germany). Mouse and rabbit calbindin antibodies to calbindin D-28K (calbindin) were used to identify horizontal cells in mammalian retina (Uesugi et al., 1992; Peichl and González-Soriano, 1994; Raven and Reese, 2002; Hirano et al., 2007). A mouse monoclonal antibody to cellular retinaldehyde-binding protein (CRALBP) was used to identify Müller cells and retinal pigmented epithelial cells (Bunt-Milam and Saari, 1983). This CRALBP antibody is to human recombinant CRALBP, and it recognizes a single band on Western blot of human recombinant CRALBP (ab15051; Abcam Inc., Cambridge, MA). A mouse monoclonal antibody to the calcium-activated, phospholipid-dependent protein kinase C (PKC) was used to identify rod bipolar cells (Ghosh et al., 2001; Haverkamp et al., 2003). A sheep polyclonal antibody to the N-terminus of the transcription factor Chx10 was used to identify bipolar cell bodies (AB9016; Millipore Corporation, Temecula, CA; Chow et al., 2004; Dorval et al., 2006; Nickerson et al., 2007). All of the antibodies in this study have been used in rodent retina, and additional information is provided in Table 1.

Antibody characterization

Anti-GAT-1—Anti-GAT-1 recognizes a single band of molecular size 67 kD from both mouse brain and retina homogenates in Western blots (Fig. 1); the molecular size is consistent with previous studies (Guastella et al., 1990;Pow et al., 2005). Previous studies have shown that the GAT-1 antibody (346) detects a single band (67 kD) in Western blots of oocytes transfected with GAT-1 cDNA (Corey et al., 1994). Antibody specificity for the immunostaining experiments was determined by preadsorption of the GAT-1 antibody with its cog-nate peptide, GAT-1588-599 (QAGSSASKEAYI), which was used for immunization (Johnson et al.,

1996). All specific GAT-1 immunostaining was eliminated after preadsorption with the cognate peptide for both the postnatal and the adult retinas.

Anti-GAT-3—Anti-GAT-3 recognizes a single band at 71 kD from both mouse brain and retina homogenates in Western blots (Fig. 1). The molecular size is consistent with previous studies using other GAT-3 antibodies, which detect a single band at 71 kD in Western blots of rat brain and retina (Ikegaki et al., 1994;Honda et al., 1995;Pow et al., 2005). Antibody specificity for the immunostaining experiments was determined by preadsorption of the GAT-3 antibody with its cognate peptide, GAT-3607-627 (CEAKVKGDGTISAITEKETHF), which was used for immunization (Johnson et al., 1996). All specific GAT-3 immunostaining was eliminated after preadsorption with the cognate peptide for both the postnatal and the adult retinas.

Anti-VGAT—Anti-VGAT recognizes a single band of the expected molecular size, 57 kD (McIntire et al., 1997; Sagné et al., 1997), in Western blots of mouse brain and retina (Fig. 1). Furthermore, preadsorption of this antibody with the VGAT N-terminus peptide, VGAT a.a. 75–87 (AEPPVEGDIHYQR), that was used for immunization eliminated the VGAT signal in Western blots (Synaptic Systems data sheet) and specific immunolabeling produced by VGAT at 1:1,000 on mouse retina sections at peptide concentrations of 10^{-5} to 10^{-7} M (data not shown).

Anti-VGAT-N2—Anti-VGAT-N2 recognizes a single band of the expected molecular size in Western blots of rat brain and PC-12 cells stably expressing VGAT (Chaudhry et al., 1998).

Anti-calbindin (Ms)—Numerous antibodies against calbindin D-28K, including this one, have been used to label horizontal cells and DB3 bipolar cells in mammalian retinas (Haverkamp and Wässle, 2000). It recognizes calbindin D-28K (28 kD) by immunoblot analysis (data sheet from Sigma-Aldrich, St. Louis, MO).

Anti-calbindin (Rb)—This antiserum was produced against rat recombinant calbindin D-28K. This antibody detects 28-kD calbindin on Western blots and has 10% cross-reactivity with calretinin (data sheet from Swant, Belinzona, Switzerland).

Anti-CRALBP—CRALBP is a widely used Müller cell marker in the retina (Bunt-Milam and Saari, 1983; Johnson et al., 1997). This CRALBP antibody is to human recombinant CRALBP, and it recognizes a single band on Western blot of human recombinant CRALBP (Abcam Inc. data sheet).

Anti-PKC—PKC is a well-characterized marker for rod bipolar cells in retina of many species (Haverkamp and Wässle, 2000). This monoclonal antibody (clone MC5) was raised against PKC (Mr 79–80 kD) purified from bovine brain. The PKC antibody recognized the purified PKC protein as well as an 80-kD band from whole-cell extracts of rat glioma and murine NIH3T3 cell lines on Western blots and specifically immunoprecipitated PKC from cell lysates of 328 glioma and SVK 14 cell lines. The epitope was mapped by ELISA using a peptide corresponding to a.a. 296–317 of PKC and shorter fragments thereof to the hinge region (a.a. 304–309 KFEKAK), close to or at the trypsin cleavage site of PKC (Young et al., 1988). Binding of the antibody was completely blocked by the full-length peptide but was not blocked by a nonrelated peptide (Young et al., 1988). This antibody reacts with PKC-alpha/ beta-1/ beta-2 isoforms (Biodesign International data sheet).

Anti-Chx10—This polyclonal antiserum was produce against the N-terminus of the recombinant human Chx10 protein (Millipore data sheet) in sheep. It was used to identify

bipolar cell bodies (Chow et al., 2004; Dorval et al., 2006; Nickerson et al., 2007). Chx10 was also expressed in some Müller cells, as reported previously (Rowan and Cepko, 2004).

Western blotting

Western blotting with the GAT-1, GAT-3, and VGAT antibodies was carried out to confirm the presence of these transporters in the mouse retina and to characterize further the specificity of these transporter antibodies. The retina and brain were homogenized in homogenizing buffer (T-PER Tissue Protein Extraction Reagent, No. 78510; Pierce Chemical, Rockford, IL) containing proteinase inhibitor cocktail (No. 1836153001; Roche Applied Science, Indianapolis, IN), 1% Triton X-100, and 2% glycerol. Protein concentrations were determined by using Bio-Rad Protein Assay Dye Reagent (No. 500-0006; Bio-Rad Laboratories, Hercules, CA), and 10–20 μg of total protein from brain and retina homogenates was run on a 4–20% polyacrylamide gel in an EC mini-gel electrophoresis apparatus, with ColorPlus Prestained Protein Marker (No. P7709V; New England Biolabs, Ipswich, MA) for molecular weight reference. The proteins were subsequently transferred to a polyvinylidene fluoride (PVDF) membrane (Hybond-P PVDF membrane, No. RPN1416F; Amersham Biosciences, Piscataway, NJ) in an EC tank transphor unit (Amersham Biosciences). Membranes were probed with antibodies against GAT-1 (1:1,000), GAT-3 (1:1,000), and VGAT (1:1,500) diluted in blocking buffer containing 25 mM Tris Cl (pH 7.5), 150 mM NaCl, 0.1 mM phenylmethanesulphonyl fluoride (PMSF), 2 mM EDTA, 5% nonfat dry milk, and 0.05% Tween-20. Labeled band was revealed by using species-specific horseradish peroxidase (HRP)-conjugated secondary antibody, goat anti-rabbit (No. 31460; Pierce Chemical) for GAT-1 and GAT-3 and goat anti-mouse for VGAT (No. 31430; Pierce Chemical) diluted in blocking buffer and detected with enhanced chemiluminescence (SuperSignal West Femto Maximum Sensitivity Substrate, No. 34095; Pierce Chemical) on Kodak BioMax light film.

The GAT-1 (346O) and GAT-3 (374D) antibodies recognized a single band of the expected molecular size, 67 kD and 71 kD (Guastella et al., 1990; Liu et al., 1993), respectively, in Western blots of mouse brain and retina (Figure 1). Previous studies have shown that the GAT-1 antibody (346) detects a single band (67 kD) in Western blots of oocytes transfected with GAT-1 cDNA (Corey et al., 1994). Furthermore, other GAT-1 and GAT-3 antibodies detect a single band at 67 kD and 71 kD, respectively, in Western blots of rat brain and retina (Ikegaki et al., 1994; Honda et al., 1995; Pow et al., 2005).

The mouse monoclonal VGAT antibody (No. 131 011) recognizes a single band of the expected molecular size, 57 kD (McIntire et al., 1997; Sagné et al., 1997), in Western blots of mouse brain and retina (Figure 1). Furthermore, preadsorption of this antibody with the VGAT N-terminus peptide $VGAT_{75–87}$ (AEPPVEGDIHYQR) that was used for immunization eliminated the VGAT signal in Western blots (Synaptic Systems data sheet). The rabbit polyclonal VGAT-N2 antibody recognizes a single band of the expected molecular size in Western blots of rat brain and PC-12 cells stably expressing VGAT (Chaudhry et al., 1998). A set of other antibodies direct to VGAT, including a rabbit antibody to $VGAT_{75–87}$, also detected a single band at 57 kD in Western blots with tsA201 cells transfected with VGAT cDNA, whereas no signal was detectable in mock-transfected cells (Takamori et al., 2000).

Immunohistochemistry

Immunohistochemical labeling was carried out by using the indirect immunofluorescence method (Hirano et al., 2005, 2007). Retinal sections were incubated in 10% normal goat serum (NGS), 1% bovine serum albumin (BSA), 0.5% Triton X-100, and 0.05% sodium azide in 0.1 M phosphate-buffered saline (PBS), pH 7.4, for 1 hour at room temperature. The blocking solution was replaced by the primary antibody diluted in 3% NGS, 1% BSA, 0.5% Triton X-100, and 0.05% sodium azide in PBS and incubated overnight at 4°C in a humidified

chamber. After washes in 0.1 M phosphate buffer (PB; pH 7.4), the sections were incubated for 30–60 minutes at room temperature in secondary antibody mix and diluted in the same solution as the primary antibody, except that sodium azide was omitted. The primary antibody/antigen complex was detected by using the appropriate secondary antibodies conjugated to Alexa 488, Alexa 568, or Alexa 594 at dilution of 1:500 or 1:1,000 (Invitrogen, Carlsbad, CA). After washes in 0.1 M PB, the sections were mounted in Aqua Poly/Mount (Poly-sciences, Warrington, PA). Retinal sections used for these experiments were obtained from both the central and the peripheral retina.

The optimal working dilutions of these antibodies were determined in adult retina, and the developmental studies were usually performed at a concentration higher than that used for the adult retina. The GAT-1, GAT-3, and VGAT antibodies were used as follows: for P0–P10 retinas, GAT-1 and GAT-3 were used at 1:100, and VGAT and VGAT-N2 were used at 1:1,000; for P15–P30 and adult retinas, GAT-1 and GAT-3 were used at 1:500, and VGAT and VGAT-N2 were used at 1:1,000.

The mouse monoclonal and rabbit polyclonal calbindin antibodies were used at 1:2,500 and 1:8,000, respectively, in both postnatal and adult retina. The CRALBP and PKC antibodies were used at 1:1,000 and 1:200, respectively, in adult retina. The Chx10 antibody was used at 1:2,500 in the adult retina. The immunostaining patterns in this study matched earlier descriptions of the calbindin, CRALBP, PKC, and Chx10 immunostaining patterns in mammalian retina (Bunt-Milam and Saari, 1983; Peichl and González-Soriano, 1994; Haverkamp and Wässle, 2000; Ghosh et al., 2001; Haverkamp et al., 2003; Chow et al., 2004; Rowan and Cepko, 2004; Morrow et al., 2008).

Antibody specificity for the immunostaining experiments was determined by preadsorption of the GAT-1 and GAT-3 antibodies with their respective cognate peptides; GAT-$1_{588–599}$ (QAGSSASKEAYI) and GAT-$3_{607–627}$ (CEAKVKGDGTISAITEKETHF), which were used for immunization (Johnson et al., 1996). Preadsorption experiments were conducted with P3 and P5 retinas at 1:100 and adult retina at 1:500 for GAT-1 and GAT-3. For this control, the primary antibody was first incubated with 7 μM GAT-1 or GAT-3 C-terminus peptide for 30 minutes at room temperature before being used. All specific GAT-1 or GAT-3 immunostaining was eliminated after preadsorption with the cognate peptides for both the postnatal and the adult retinas. GAT-1 and GAT-3 antibodies were tested in preadsorption experiments with cognate peptides of the other GAT in a previous study. GAT-1 immunostaining is not reduced when GAT-1 antibodies are incubated with 10^{-5} M GAT-3 C-terminus peptide, and GAT-3 immunostaining is not reduced when GAT-3 antibodies are incubated with 10^{-5} M GAT-1 C-terminus peptide (Johnson et al., 1996). Other plasma membrane transporter C-terminus peptides, including rat GAT-2 and rat glycine plasma membrane transporter-1, do not reduce immunostaining (Johnson et al., 1996).

The Synaptic Systems data sheet did not provide the specificity of the monoclonal VGAT antibody for immunohisto-chemistry. However, by Western blot analysis, this antibody is specific for VGAT (Fig. 1). Other studies have used the monoclonal VGAT antibody and report VGAT immunoreactivity in axonal endings (Tafoya et al., 2006;Baer et al., 2007). Anti body specificity of the rabbit polyclonal VGAT-N2 antibody was previously shown by elimination of immunostaining with an N-terminus VGAT fusion protein in the rat brain (Chaudhry et al., 1998) and in the retinas of rat and mouse (Cueva et al., 2002). The mouse monoclonal VGAT and rabbit polyclonal VGAT-N2 antibodies revealed immunostained amacrine and horizontal cells in the mouse, rat, and monkey retina (Haverkamp et al., 2000;Cueva et al., 2002). Furthermore, the immunostaining pattern in the mouse retina using these antibodies is the same as that observed in the mouse, rat, and human retina with a rabbit polyclonal C-terminus VGAT

antibody and a fourth rabbit polyclonal N-terminal VIAAT antibody (Cueva et al., 2002;Jellali et al., 2002).

For double-label immunostaining studies, one of the two primary antibodies was omitted during the primary incubation step as a control. In this case, only the immunoreactivity for the remaining primary antibody and nonspecific background staining were detected. All antibodies were tested on mouse retina as single-labeling experiments at least three times to confirm specificity and optimize concentration prior to performing any double-labeling experiments.

Confocal imaging

Images of retinal sections were acquired using a Zeiss laser scanning microscope 510 Meta (Zeiss, Thornwood, NY) Plan Neofluar ×40 1.3-NA oil objective or a C-Apochromat ×40 1.2-NA water objective. To identify fluorescent signals, different lasers were used for excitation: for Alexa 488, the 488-nm argon laser line was used, and for Alexa 568, the 543-nm HeNe laser line was used. During acquisition of signals from double-labeled specimens, the scans were collected sequentially to prevent spectral bleed-through. Specific bandpass filters were used to achieve proper separation of signals (for single labeling with Alexa 488, 488/505LP; for Alexa 568, 543/560LP; for double labeling, 488/505-530, 543/560LP). Most images were acquired at a resolution of 2,048 × 2,048 as 12-bit signals. To increase the signal-to-noise, images were averaged online (e.g., n = 4), and the scan speed and photomultiplier detector gain were decreased. Most confocal images were acquired at an approximate optical thickness of 0.3 or 1.0 μm, usually ~0.7–1.0 Airy units. For projections, typically three to eight optical sections were acquired with an average total thickness of 1–8 μm and compressed for viewing. Digital confocal images were saved as Zeiss LSM files, and final publication-quality images were exported in the TIFF format using Zeiss LSM 510 Meta software version 3.2 (Zeiss Ltd., Thornwood, NY). All images were processed, adjusted for brightness and contrast, and resized to 300 dpi in Adobe Photoshop 7.0 (Adobe Systems Inc., Mountain View, CA).

RESULTS

The spatial and temporal patterns of GAT-1, GAT-3, and VGAT expression were evaluated at multiple ages between P0 and P20 and at several adult ages from P30 to 2 years. Both central and peripheral retinal regions were evaluated. Overall, GAT-1, GAT-3, and VGAT immunostaining was present at all postnatal ages in all retinal areas. Immunostaining was absent in control sections (data not shown).

GAT-1 expression

GAT-1 immunoreactivity was in the inner retina at P0 and at all stages of postnatal development (Figure 2). Immunoreactivity was distributed mainly at or near the plasma membrane of amacrine cells located in the INL. Less frequently occurring, small immunoreactive cell bodies were also in the GCL. Immunoreactive processes and small puncta were distributed mainly to the IPL. GAT-1-immunoreactive somata were not present in the middle of the INL, corresponding to the region where most bipolar cell bodies are located. This immunostaining pattern is consistent with GAT-1 expression by amacrine cells and its variants, including displaced amacrine and inter-plexiform cells. The adult pattern of GAT-1 immunostaining was established during the early part of the third postnatal week.

Inner retina—GAT-1 immunostaining in the inner retina was weak at P0, and immunostaining intensity increased markedly from P0 to P5 in the IPL (Figure 2A,B). At both P0 and P5, GAT-1 immunoreactivity was in many small cell bodies located in the proximal INL and a few small cell bodies in the GCL. These are likely to be amacrine and displaced amacrine cells, respectively, based on their size and appearance (Figure 2A,B). At P0 and P5,

immunostained cell bodies and processes had a grainy appearance. In many cases, the primary process entering the IPL had a very high level of immunoreactivity, as did some of the processes and puncta in the IPL. GAT-1-immunoreactive processes and puncta were distributed across the IPL at both of these ages. In addition, at P0, there was weak GAT-1 immunoreactivity in the nerve fiber layer (NFL) and along the margin of the inner limiting membrane (ILM). At P5, GAT-1 immunoreactivity was reduced in the NFL and was not apparent at the margin of the ILM.

There was also an increase in GAT-1 immunoreactivity in the inner retina from P5 to P10 (Figure 2B,C); GAT-1 immunostained cell bodies were more prominent and distributed to the first two or three cellular rows of the proximal INL. At P10, P15, and P20, there were numerous immuno-reactive amacrine cells in the first two or three cellular rows of the proximal INL (Figure 2C–E). In addition, there were displaced amacrine cells in the GCL. The amacrine and displaced amacrine cells were similar in size, and they were characterized by a continuous distribution of GAT-1 immunoreactivity around their somata at or near the plasma membrane, with little or no cytoplasmic immunostaining. A similar number of GAT-1-immunolabeled somata appeared to be present in the proximal INL from P10 to P30 and older adult retinas. However, there may be some differences in cell number and density at these different postnatal ages, because the retina is growing during the postnatal period, and a rigorous quantification of the number of GAT-1 somata was not conducted. Numerous strongly GAT-1 immunoreactive processes and puncta were distributed to all IPL lamina from P10 to P30, similar to the pattern observed in adult retina. Finally, weak GAT-1 immunostaining was present in the GCL and NFL at P10 and older ages.

Outer retina—GAT-1 immunoreactivity appeared to be absent in the neuroblast layer (NBL) at P0 (Figure 2A). At P15, very weak GAT-1 immunostaining was detected in radially oriented processes that ended at the outer limiting membrane (OLM; Figure 2C). Weakly GAT-1-immunostained processes were in the ONL and diffuse immunostaining was in the OPL at all older postnatal retinas and in adult retina (Figure 2D–F). GAT-1 immunoreactivity was just detectable at antibody dilutions used to demonstrate robust GAT-1 immunostaining in the inner retina. At higher GAT-1 antibody concentrations, specific GAT-1 immunostaining is observed in the outer retina, as reported earlier for the adult rat retina (Johnson et al., 1996). Furthermore, GAT-1 immunostaining is not likely to be due to cross-reactivity with GAT-3, because GAT-1 antibody immunostaining is not affected by preadsorption with the C-terminus GAT-3 peptide (Johnson et al., 1996).

The cellular localization of GAT-1 immunoreactivity in the distal INL and OPL was also evaluated by using antibodies to GAT-1 and the horizontal cell marker calbindin or the Müller cell marker CRALBP in P3, P5, and adult (P48) retinas (Figs. 3, 4). Diffuse GAT-1 immunostaining in the OPL was observed with a higher antibody concentration than that used to demonstrate GAT-1 expression by amacrine cells. In the adult retina OPL, the GAT-1 immunostaining pattern had a polygonal appearance (Figs. 3D, 4E), which circumscribe triad synapses, consisting of photoreceptor terminals and bipolar and horizontal cell processes. In the postnatal and adult retinas, calbindin-immunoreactive horizontal cell tips were surrounded by the faint GAT-1 immunostaining (Fig. 3F). Furthermore, in the adult retina, the GAT-1 immunoreactivity in the OPL was coexpressed with CRALBP immunoreactivity (Fig. 4). Together, these observations indicate that, in the OPL, GAT-1 immunoreactivity was restricted to Müller cell processes.

GAT-3 expression

GAT-3 immunoreactivity was present at P0 and at all of the later stages of postnatal development (Fig. 5). GAT-3 immunostaining was located at or near the plasma membrane of

cell bodies located in the proximal and middle of the INL. Immunoreactive processes were present in the IPL. GAT-3-immunoreactive processes spanning the retina from the ILM to the OLM were readily apparent at P15 and older ages. Overall, this immunostaining pattern is consistent with GAT-3 expression by amacrine and Müller cells. The adult pattern of GAT-3 immunostaining was established during the third post-natal week.

Inner retina—At P0, GAT-3 immunoreactivity in the inner retina was weak, and immunoreactivity increased dramatically from P0 to P5. At both P0 and P5, low levels of GAT-3 immunoreactivity were present in a few small cell bodies located in the middle and proximal layers of the INL (Fig. 5A,B). At P0, a few immunostained processes were distributed to the IPL, and they were characterized by a grainy appearance. Some immunoreactive processes also surrounded cell bodies in the GCL and others were distributed to the NFL, adjacent to the ILM (Fig. 5A). In contrast, at P5, there were high levels of GAT-3 immunostaining in the IPL and in Müller cell endfeet in the GCL and NFL (Fig. 5B).

There appears to be an increase in the level of GAT-3 immunoreactivity from P5 to P10 (Fig. 5B,C). At P10, P15, and P20, GAT-3-immunoreactive amacrine and Müller cell bodies were in the proximal and middle INL, respectively (Fig. 5C–E). The small amacrine cell bodies gave rise to a primary process that entered the IPL. Numerous strongly immunostained processes and puncta were distributed to all IPL lamina from P10 to P30, similar to the pattern observed in adult retina. Numerous Müller cells gave rise to processes that spanned the retina from the ILM to the OLM beginning at P10. Müller cell processes containing GAT-3 immunoreactivity were prominent in all retinal layers, and radially oriented Müller cell processes were observed in the INL and ONL (Fig. 5C–F). In addition, in P15, P20, and adult retinas, there were high levels of GAT-3 immunoreactivity in Müller cell processes and endfeet in the GCL and NFL adjacent to the ILM (Fig. 5D–F).

Double-labeling experiments with GAT-3, PKC, and Chx10 antibodies were used to determine whether bipolar cells contain GAT-3 immunoreactivity (Fig. 6). GAT-3 immunoreactivity was not localized to the bipolar cell somata or processes identified by PKC immunostaining (Fig. 6A–F) or in bipolar cell bodies identified by Chx10 immunostaining (Fig. 6G–L). GAT-3-immunoreactive somata were distributed among the PKC and Chx10-immunoreactive bipolar cells, and GAT-3-immunoreactive processes surrounded bipolar cell and photoreceptor somata in the INL and ONL (Fig. 6). Furthermore, Chx10 was also expressed in some Müller cells, as reported previously (Rowan and Cepko, 2004), and, in these cases, the Müller cell bodies contained both GAT-3 and Chx10 immunoreactivities. Multiple-label experiments with GAT-3, Chx10, and CRALBP antibodies confirmed the presence of GAT-3 in Chx10 and CRALBP-expressing Müller cell bodies (data not shown).

Outer retina—At P0 and P5, GAT-3 immunoreactivity was at the OLM, and in addition there are a few weakly immunostained processes outlining cell bodies in the outer NBL near the OLM (Fig. 5A). In addition, weakly immunostained processes outlined cell bodies in the INL and ONL, and these processes terminated at the OLM. Immunostaining levels in the INL and OPL were increased markedly at P10 (Fig. 5B,C).

The increase of the GAT-3 immunoreactivity in the Müller cell processes in the ONL and OPL appears to be a result of both an increased level of GAT-3 immunoreactivity in individual Müller cell processes and an increased number of immunoreactive Müller cells processes. The adult pattern of GAT-3 immunostaining in the outer retina was established during the beginning of the third postnatal week.

The cellular localization of GAT-3 immunoreactivity in the distal INL and OPL was evaluated by using antibodies to GAT-3 and calbindin or CRALBP in P3, P5, and adult (P48) retinas

(Figs. 7, 8). In the postnatal and adult retinas, calbindin-immunoreactive horizontal cell tips were surrounded by GAT-3-immunoreactive processes (Fig. 7). In the adult retina, GAT-3 and CRALBP immunoreactivities were co-expressed in processes distributed to the OPL (Fig. 8). Both GAT-3 and CRALBP immunostaining in the OPL had a polygonal appearance, which filled the space around the photoreceptor terminals, bipolar cell dendrites, and horizontal cell processes. In addition, both GAT-3 and CRALBP immunoreactivities were coexpressed in Müller cell somata and their processes, which spanned the radial thickness of the retina from the ILM to the OLM. These observations also indicate that GAT-3 immunoreactivity was restricted to Müller cell processes in the OPL.

VGAT expression

VGAT immunoreactivity was in the inner retina at P0 and at all of the later stages of postnatal development (Fig. 9). Low levels of immunoreactivity were found in the cytoplasm of amacrine cell bodies, and high levels of immunoreactivity were observed in numerous processes distributed to the IPL. Weak VGAT immunostaining was detected in the OPL at P5 in horizontal cells and their processes (Fig. 9B). VGAT immunoreactive somata were not present in the middle of the INL, corresponding to the region where most bipolar cell bodies are located. This immunostaining pattern is consistent with VGAT expression by amacrine and horizontal cells (Cueva et al., 2002;Jellali et al., 2002;Johnson et al., 2003). The adult pattern of VGAT immunostaining was established at the end of the second postnatal week.

Inner retina—At P0, low levels of VGAT immunoreactivity were distributed across the IPL (Fig. 9A). Low levels of immunoreactivity were also present in the cytoplasm of cell bodies localized to the INL and GCL. Nonspecific immunostaining was present along the margin of the ILM at P0 and P5, perhaps because of the vitreous, which was not removed in retinas collected at P0, P3, and P5. VGAT immunostaining was characterized by a grainy appearance in these layers. At P5, there was a marked increase in the level of VGAT immunostaining in the IPL compared with P0. VGAT immunoreactivity was present in processes and puncta that were distributed across the IPL. Some amacrine cell bodies in the proximal INL also had a low level of VGAT immunoreactivity.

At P10, P15, and P20 there were numerous immunoreactive amacrine cell bodies in the first two or three cellular rows of the proximal INL (Fig. 9C–E). Very low levels of VGAT immunoreactivity characterized these amacrine cells. VGAT-immunoreactive primary processes that entered the IPL contained higher levels of immunoreactivity. The number of VGAT-immunoreactive amacrine cells at these ages appears to be similar to the number of VGAT-expressing amacrine cells at P30 and older adult ages. Numerous, strongly immunoreactive processes and puncta were found in all IPL laminae at P10, P15, and P20 as well as in adults (Fig. 9C–F).

Outer retina—At P0, VGAT immunoreactivity appeared to be absent in the outer retina and the overlying NBL (Fig. 9A). At P3 and P5, weak VGAT immunostaining was detected in horizontal cell processes and tips (Fig. 9B). At P10, VGAT immunoreactivity was distributed mainly to horizontal cell processes and their tips, which had a punctate appearance in the OPL (Fig. 9C). VGAT immunostaining of horizontal cell bodies was weak. Furthermore, at P10 and P15, the intensity of immunostaining in horizontal cell processes and tips appeared to be greater than the intensity of immunostaining at P20 and adults (Fig. 9C–F). The adult pattern of VGAT immunostaining in the outer retina was established at the end of the second postnatal week (Figs. 9D–F, 10).

The cellular localization of VGAT immunoreactivity to horizontal cell processes and tips was confirmed by using antibodies to VGAT and calbindin in P5 and adult retina (Fig. 10). VGAT

immunoreactivity is expressed in calbindin-containing horizontal cell bodies, terminals, and processes in the OPL, which is consistent with observations in the adult mouse and rat retina (Cueva et al., 2002;Jellali et al., 2002;Johnson et al., 2003).

DISCUSSION

These studies describe the developmental expression of plasma membrane and vesicular GABA transporters in the mouse retina. The plasma membrane transporter GAT-1 was preferentially expressed by amacrine and displaced amacrine cells and their processes in the IPL. In addition, Müller cells contained low levels of GAT-1 immunoreactivity. Müller cells also showed prominent GAT-3 immunoreactivity in their somata and processes, spanning the retina from the ILM to the OLM. In the inner retina, amacrine cells also expressed GAT-3 immunoreactivity, with numerous processes and puncta in the IPL. A high density of immunoreactive processes for both GAT-1 and GAT-3 was present in all laminae of the IPL. The vesicular GABA transporter VGAT was strongly expressed by amacrine and displaced amacrine cell processes in the IPL, whereas weaker VGAT immunoreactivity occurred in horizontal cells and their processes in the OPL. Unlike the case in cat and primate retina (Agardh et al., 1987; Pourcho and Owczarzak, 1989; WÄssle and Chun, 1989; Grünert and WÄssle, 1990; Kao et al., 2004), bipolar cells in mouse retina do not appear to express the plasma membrane or vesicular GABA transporters, but rather GAT-3-containing Müller cell processes appeared to wrap around bipolar cell bodies in the INL (Fig. 6). These latter observations are consistent with an earlier study of VGAT expression in the developing mouse retina (Johnson et al., 2003).

All three transporters were present at low levels in the inner retina at birth (P0), suggesting that amacrine and Müller cells initially express these transporters during late embryonic stages. In the inner retina, transporter expression levels increased markedly from P0 to P5 and P10, following the final stages of amacrine and Müller cell birth (Young, 1985; Cepko et al., 1996; Donovan and Dyer, 2005). Transporter expression in the outer retina lagged behind the inner retina, and the mature immunostaining pattern was established during the end of the second and the beginning of the third postnatal weeks. Together, these observations suggest that these transporter systems are mature and functional at the end of the second postnatal week at about the time of eye opening, which happens between P12 and P14.

GAT-1 and GAT-3 expression in the developing retina

Amacrine cells—The prominent expression of GAT-1 and GAT-3 by amacrine and Müller cells and their processes supports the idea that these transporters have a major role in regulating GABA levels in the inner retina. The presumptive IPL during the first postnatal week contains numerous GAT-1-and GAT-3-immunostained processes and puncta. Within the IPL, GAT-1 expression appears to dominate early in development, with GAT-3 expression reaching similar levels by P30. In the INL, there were numerous GAT-1-immunoreactive amacrine cell bodies that were adjacent in the first two or three cellular rows of the proximal INL. In contrast, the GAT-3-immunoreactive cell bodies appeared to be more widely spaced and fewer in number than the GAT-1-immunoreactive cells. We cannot tell with certainty whether GAT-1 and GAT-3 are expressed in the same amacrine cells, because both the GAT-1 and the GAT-3 antibodies that we used were raised in rabbits. Furthermore, the high density of labeled processes in the IPL for both GAT-1 and GAT-3 makes it impossible to evaluate their colocalization within individual processes at the light microscopic level.

Müller cells—In contrast to the strong immunolabeling in amacrine cells by P5, weak GAT-1 immunostaining does not become readily apparent in Müller cells until P15. This observation likely reflects the low level of GAT-1 immunoreactivity in Müller cells. Low levels of GAT-3

immunostaining in the retina were detected at P0 and P5, where immunoreactivity was mainly distributed to the IPL, but was present as well in the NFL and ILM and in the NBL adjacent to the OLM. Radially oriented GAT-3-immunoreactive processes were also distributed to the NBL, and these were most prominent near the OLM. Overall, this expression pattern suggests that it is the Müller cells that express GAT-3 during the first postnatal week, which is consistent with their differentiation and functional maturation between E21 and P11 (Young, 1985; Rapaport et al., 1996). Finally, during the first postnatal week, Müller cell somata in the NBL were not immunolabeled, indicating a nondetectable and likely low level of GAT-3 immunoreactivity in their somata. In contrast, the GAT-3 immunostaining in Müller cell somata and their processes becomes well established during the early part of the second postnatal week.

GAT-1 and GAT-3 are coexpressed in Müller cells and their processes, although at very different levels: GAT-1 levels are lower at all ages compared with GAT-3 levels. The presence of very weak GAT-1 immunostaining in Müller cells and their processes at all postnatal ages is consistent with reports of weak GAT-1 immunoreactivity in Müller cells in adult rat and guinea pig retinas (Johnson et al., 1996; Biedermann et al., 2002). Low levels of GAT-1 immunoreactivity in Müller cells are also consistent with earlier observations in the rat retina that Müller cells contain low levels of GAT-1 mRNA (Brecha and Weigmann, 1994). Finally, antibody preadsorption studies showed no cross-reactivity between the GAT-1 and GAT-3 antibodies in a previous study (Johnson et al., 1996), further suggesting that the colocalization of GAT-1 and GAT-3 is not a technical artifact. The localization of GAT-1 to Müller cells suggests that this transporter functions to remove GABA from the synaptic cleft and extracellular space. Furthermore, the low expression of GAT-1 immunoreactivity in Müller cells and their processes in the GCL and NFL and distal INL, OPL, and ONL, compared with the expression of GAT-3 immunoreactivity, suggests that GAT-1 is likely to have a minor overall influence on GABA uptake and neurotransmission in these retinal regions. The presence of both GAT isoforms likely confers a greater range of control of GABA concentration as a result of the different functional properties of the GAT iso-forms (Borden, 1996) and the differential regulation of surface expression and transport activity by PKC and protein phosphorylation (Wang and Quick, 2005; Quick, 2006; Hu and Quick, 2008).

The idea that Müller cells have a major functional role in removing GABA from the synaptic clefts and regulating GABA in the extracellular space suggests that it would influence high-affinity $GABA_A$ and $GABA_C$ receptors located away from GABA release sites (Ichinose and Lukasiewicz, 2002; Hull et al., 2006). The immunohistochemical findings complement electrophysiological studies reporting that GAT-1 activity shapes $GABA_A$- and $GABA_C$-mediated inhibitory responses in the adult retina (Ichinose and Lukasiewicz, 2002; Hull et al., 2006).

VGAT expression in the developing retina

Similarly to the GABA plasma membrane transporters, weak VGAT immunostaining was detected at P0 in the inner retina. At P5 and older ages, VGAT immunoreactivity was expressed in amacrine and horizontal cells and their processes in the IPL and OPL, respectively (Johnson et al., 2003), suggesting that vesicular GABA transmission occurs during the first postnatal week. In agreement, bicuculline-sensitive inhibitory postsynaptic currents (IPSCs) are first observed at E17 in mouse ganglion cells, and functional $GABA_A$ receptors were present earlier, at E15 (Unsoeld et al., 2008). Congruent with these findings is a low frequency of spontaneous IPSCs in mouse ganglion cells at P7, followed by an increase in the average frequency of spontaneous IPSCs during the second and third postnatal weeks (Johnson et al., 2003).

In the developing and adult retina, VGAT immunoreactivity is localized principally to amacrine cell processes in all IPL laminae. This immunostaining pattern is similar to the distribution of GAT-1 and GAT-3 processes in the IPL. In addition, weak VGAT

immunostaining was detected in horizontal cell bodies and processes beginning in the first postnatal week, and this immunostaining becomes more prominent during the second postnatal week. The expression of VGAT in horizontal cells overlaps with the expression of GABA and GAD in horizontal cells and their processes (Schnitzer and Rusoff, 1984; Versaux-Botteri et al., 1989; Eliasson et al., 1997; Fletcher and Kalloniatis, 1997; Yamasaki et al., 1999; Dkhissi et al., 2001). GAD immunoreactivity in developing horizontal cells in mouse retina was greatest between E17 and P3 (Schnitzer and Rusoff, 1984), before prominent expression of VGAT immunoreactivity in the OPL.

VGAT mediates high-affinity uptake of GABA and glycine into synaptic vesicles (McIntire et al., 1997; Sagné et al., 1997; Takamori et al., 2000). The expression of VGAT, which has been localized to synaptic vesicles (Chaudhry et al., 1998; Dumoulin et al., 1999; Takamori et al., 2000), correlates with ultrastructural descriptions of the presence of synaptic vesicles in amacrine cell processes and at conventional synapses in the IPL and in horizontal cell processes (Olney, 1968; Blanks et al., 1974; Fisher, 1979). The presence of vesicles and VGAT suggests the possibility that Ca^{2}+-dependent vesicular release of GABA and/or glycine occurs during the first postnatal week. Bicuculline-sensitive spontaneous PSCs at E17 (Unsoeld et al., 2008) and spontaneous IPSCs at P7 in mouse ganglion cells (Johnson et al., 2003), indicate that GABAergic and/or glycinergic vesicular release is occurring in the inner retina by these times.

Functional role of GABA in the developing retina

In the developing nervous system, GABA mediates a broad spectrum of trophic effects that influence cell survival, dendritic outgrowth and differentiation, and synaptogenesis (for reviews see Ben-Ari, 2002; Owens and Kriegstein, 2002; Represa and Ben-Ari, 2005). The presence of GABA, GAD, and the GABA plasma membrane and vesicular transporters in the retina during the late prenatal period and during the first 2 postnatal weeks (Schnitzer and Rusoff, 1984; Versaux-Botteri et al., 1989; Messersmith and Redburn, 1992; Fletcher and Kalloniatis, 1997; Yamasaki et al., 1999; Dkhissi et al., 2001), before visually evoked retinal activity occurs, is consistent with the idea that GABA has a trophic role in the developing retina. For instance, in the rabbit OPL, during the first post-natal week, GABA originating from horizontal cells is reported to have a strong influence on cone photoreceptor number and position as well as the synaptogenesis and the formation of cone pedicles (Messersmith and Redburn, 1990, 1993; Huang et al., 2000). In vitro evidence for GABA's trophic action in the retina includes its influence on neurite outgrowth, differentiation, and synaptogenesis in neuronal cultures of chick retina (Spoerri, 1988). Furthermore, in the developing chick retina, GABA originating from amacrine cells is reported to regulate ganglion cell dendritic motility during synapse formation (Wong and Wong, 2001). Finally, GABA signaling has been implicated in the formation and propagation of retinal waves, which are thought to influence synaptic organization and circuitry formation in the inner retina (Zheng et al., 2004; Wang et al., 2007).

In the outer retina, horizontal cell processes innervate cone photoreceptor terminals beginning at P4 and rod photoreceptor terminals at P8 (Olney, 1968; Weidman and Kuwabara, 1968; Blanks et al., 1974; Rich et al., 1997). The formation of photoreceptor synaptic triads is completed by the end of second postnatal week (Olney, 1968; Blanks et al., 1974). From E17 to P3, developing horizontal cells exhibit strong immunoreactivity for GABA and the GABA synthetic enzyme L-glutamate decarboxylase (GAD) in mouse and rat retina, whereas weak GAD immunoreactivity is seen in cell bodies adjacent to the IPL (Schnitzer and Rusoff, 1984; Versaux-Botteri et al., 1989; Eliasson et al., 1997; Fletcher and Kalloniatis, 1997; Yamasaki et al., 1999; Dkhissi et al., 2001).

In the OPL, GAT-1 and GAT-3 immunostaining encapsulates the photoreceptor terminal, bipolar cell dendrites, and horizontal cell processes (Figs. 3, 6, 7). This spatial organization correlates well with the idea that Müller cells regulate levels of extracellular GABA released from horizontal cells. The lack of GABA and GABA analogue uptake by mammalian horizontal cells is consistent with the lack of GAT expression in these cells (Ehinger, 1977;Pourcho, 1981;Agardh and Ehinger, 1982;Blanks and Roffler-Tarlov, 1982). In addition, the expression level of GAT-3 in Müller cell processes in the OPL and ONL is dramatically higher than that of GAT-1, implying that GAT-3 is the principal GABA transporter in the outer retina, and it has a strong influence on extracellular GABA levels in the OPL. Although the immunoreactivity for GAT-1 is weaker than that for GAT-3 in the outer retina, the level of GAT-1 immunoreactivity in the outer retina is highest within the OPL. These observations indicate that, unlike the case in the inner retina, where both amacrine and Müller cells show high levels of GAT-1 and GAT-3 immunoreactivities, the principal uptake mechanism for GABA is predominantly glial in the outer retina.

In summary, this study has demonstrated that the plasmalemmal GABA transporters GAT-1 and GAT-3 and the vesicular transporter VGAT are present in the mouse retina at low levels at birth and that the adult pattern of transporter expression is established during the first and second postnatal weeks. This is concomitant with the morphological development of amacrine and Müller cells; the expression of GABA, GAD_{65}, and GAD_{67}; and the establishment of synaptic circuitry in the IPL and OPL. The GAT and VGAT transporter systems appear to be functionally mature at the beginning of the third postnatal week, at about the time of eye opening.

Acknowledgments

We thank Dr. Catia Sternini for her helpful comments and suggestions on the manuscript. We also thank Dr. Richard J. Reimer, Stanford University School of Medicine, for the VGAT-N2 antibody. Finally, we thank Alex Vila and Van Nguyen for their assistance in performing some of these studies. N.C.B. is a VA Senior Career Research Scientist.

Grant sponsor: National Institutes of Health; Grant number: EY 04067; Grant number: EY 15573.

LITERATURE CITED

Agardh E, Ehinger B. (^{3}H)-muscimol, (^{3}H)-nipecotic acid and (^{3}H)-isoguvacine as autoradiographic markers for GABA neurotransmission. J Neural Transm 1982;54:1–18. [PubMed: 6286870]

Agardh E, Bruun A, Ehinger B, Ekstrom P, van Veen T, Wu JY. Gamma-aminobutyric acid- and glutamic acid decarboxylaseimmunoreactive neurons in the retina of different vertebrates. J Comp Neurol 1987;258:622–630. [PubMed: 3294928]

Attwell D, Barbour B, Szatkowski M. Nonvesicular release of neurotransmitter. Neuron 1993;11:401–407. [PubMed: 8104430]

Baer K, Burli T, Huh KH, Wiesner A, Erb-Vogtli S, Gockeritz-Dujmovic D, Moransard M, Nishimune A, Rees MI, Henley JM, Fritschy JM, Fuhrer C. PICK1 interacts with alpha7 neuronal nicotinic acetylcholine receptors and controls their clustering. Mol Cell Neurosci 2007;35:339–355. [PubMed: 17467288]

Ben-Ari Y. Excitatory actions of GABA during development: the nature of the nurture. Nat Rev Neurosci 2002;3:728–739. [PubMed: 12209121]

Biedermann B, Bringmann A, Reichenbach A. High-affinity GABA uptake in retinal glial (Müller) cells of the guinea pig: electrophysiological characterization, immunohistochemical localization, and modeling of efficiency. Glia 2002;39:217–228. [PubMed: 12203388]

Blanks JC, Roffler-Tarlov S. Differential localization of radioactive gamma-aminobutyric acid and muscimol in isolated and in vivo mouse retina. Exp Eye Res 1982;35:573–584. [PubMed: 7151891]

Blanks JC, Adinolfi AM, Lolley RN. Synaptogenesis in the photoreceptor terminal of the mouse retina. J Comp Neurol 1974;156:81–93. [PubMed: 4836656]

Borden LA. GABA transporter heterogeneity: pharmacology and cellular localization. Neurochem Int 1996;29:335–356. [PubMed: 8939442]

Borden LA, Smith KE, Hartig PR, Branchek TA, Weinshank RL. Molecular heterogeneity of the gamma-aminobutyric acid (GABA) transport system. Cloning of two novel high affinity GABA transporters from rat brain. J Biol Chem 1992;267:21098–21104. [PubMed: 1400419]

Borden LA, Dhar TG, Smith KE, Branchek TA, Gluchowski C, Weinshank RL. Cloning of the human homologue of the GABA transporter GAT-3 and identification of a novel inhibitor with selectivity for this site. Recept Channels 1994;2:207–213. [PubMed: 7874447]

Brecha NC, Weigmann C. Expression of GAT-1, a high-affinity gamma-aminobutyric acid plasma membrane transporter in the rat retina. J Comp Neurol 1994;345:602–611. [PubMed: 7962703]

Bunt-Milam AH, Saari JC. Immunocytochemical localization of two retinoid-binding proteins in vertebrate retina. J Cell Biol 1983;97:703–712. [PubMed: 6350319]

Burger PM, Hell J, Mehl E, Krasel C, Lottspeich F, Jahn R. GABA and glycine in synaptic vesicles: storage and transport characteristics. Neuron 1991;7:287–293. [PubMed: 1678614]

Casini G, Rickman DW, Brecha NC. Expression of the γ-aminobutyric acid (GABA) plasma membrane transporter-1 in monkey and human retina. Invest Ophthalmol Vis Sci 2006;47:1682–1690. [PubMed: 16565409]

Cepko CL, Austin CP, Yang X, Alexiades M, Ezzeddine D. Cell fate determination in the vertebrate retina. Proc Natl Acad Sci U S A 1996;93:589–595. [PubMed: 8570600]

Chaudhry FA, Reimer RJ, Bellocchio EE, Danbolt NC, Osen KK, Edwards RH, Storm-Mathisen J. The vesicular GABA transporter, VGAT, localizes to synaptic vesicles in sets of glycinergic as well as GABAergic neurons. J Neurosci 1998;18:9733–9750. [PubMed: 9822734]

Chen NH, Reith ME, Quick MW. Synaptic uptake and beyond: the sodium- and chloride-dependent neurotransmitter transporter family SLC6. Pflugers Arch 2004;447:519–531. [PubMed: 12719981]

Chow RL, Volgyi B, Szilard RK, Ng D, McKerlie C, Bloomfield SA, Birch DG, McInnes RR. Control of late off-center cone bipolar cell differentiation and visual signaling by the homeobox gene Vsx1. Proc Natl Acad Sci U S A 2004;101:1754–1759. [PubMed: 14745032]

Christensen H, Fykse EM, Fonnum F. Inhibition of gamma-aminobutyrate and glycine uptake into synaptic vesicles. Eur J Pharmacol 1991;207:73–79. [PubMed: 1915594]

Conti F, Minelli A, Melone M. GABA transporters in the mammalian cerebral cortex: localization, development and pathological implications. Brain Res Rev 2004;45:196–212. [PubMed: 15210304]

Corey JL, Davidson N, Lester HA, Brecha N, Quick MW. Protein kinase C modulates the activity of a cloned gamma-aminobutyric acid transporter expressed in *Xenopus* oocytes via regulated subcellular redistribution of the transporter. J Biol Chem 1994;269:14759–14767. [PubMed: 8182081]

Cueva JG, Haverkamp S, Reimer RJ, Edwards R, Wässle H, Brecha NC. Vesicular γ-aminobutyric acid transporter expression in amacrine and horizontal cells. J Comp Neurol 2002;445:227–237. [PubMed: 11920703]

Dalby NO. Inhibition of γ-aminobutyric acid uptake: anatomy, physiology and effects against epileptic seizures. Eur J Pharmacol 2003;479:127–137. [PubMed: 14612144]

De Biasi S, Vitellaro-Zuccarello L, Brecha NC. Immunoreactivity for the GABA transporter-1 and GABA transporter-3 is restricted to astrocytes in the rat thalamus. A light and electron-microscopic immunolocalization. Neuroscience 1998;83:815–828. [PubMed: 9483565]

Dkhissi O, Julien JF, Wasowicz M, Dalil-Thiney N, Nguyen-Legros J, Versaux-Botteri C. Differential expression of GAD_{65} and GAD_{67} during the development of the rat retina. Brain Res 2001;919:242–249. [PubMed: 11701136]

Dmitrieva NA, Lindstrom JM, Keyser KT. The relationship between GABA-containing cells and the cholinergic circuitry in the rabbit retina. Vis Neurosci 2001;18:93–100. [PubMed: 11347820]

Donovan SL, Dyer MA. Regulation of proliferation during central nervous system development. Semin Cell Dev Biol 2005;16:407–421. [PubMed: 15840449]

Dorval KM, Bobechko BP, Fujieda H, Chen S, Zack DJ, Bremner R. CHX10 targets a subset of photoreceptor genes. J Biol Chem 2006;281:744–751. [PubMed: 16236706]

Dumoulin A, Rostaing P, Bedet C, Lévi S, Isambert MF, Henry JP, Triller A, Gasnier B. Presence of the vesicular inhibitory amino acid transporter in GABAergic and glycinergic synaptic terminal boutons. J Cell Sci 1999;112:811–823. [PubMed: 10036231]

Durkin MM, Smith KE, Borden LA, Weinshank RL, Branchek TA, Gustafson EL. Localization of messenger RNAs encoding three GABA transporters in rat brain: an in situ hybridization study. Brain Res Mol Brain Res 1995;33:7–21. [PubMed: 8774941]

Ehinger B. Glial and neuronal uptake of GABA, glutamic acid, glutamine and glutathione in the rabbit retina. Exp Eye Res 1977;25:221–234. [PubMed: 590366]

Eliasson MJ, McCaffery P, Baughman RW, Dräger UC. A ventrodorsal GABA gradient in the embryonic retina prior to expression of glutamate decarboxylase. Neuroscience 1997;79:863–869. [PubMed: 9219949]

Fisher LJ. Development of synaptic arrays in the inner plexiform layer of neonatal mouse retina. J Comp Neurol 1979;187:359–372. [PubMed: 489784]

Fletcher EL, Kalloniatis M. Localisation of amino acid neurotransmitters during postnatal development of the rat retina. J Comp Neurol 1997;380:449–471. [PubMed: 9087525]

Gadea A, López-Colomé AM. Glial transporters for glutamate, glycine, and GABA: II. GABA transporters. J Neurosci Res 2001;63:461–468. [PubMed: 11241581]

Gammelsaeter R, Frøyland M, Aragón C, Danbolt NC, Fortin D, Storm-Mathisen J, Davanger S, Gundersen V. Glycine, GABA and their transporters in pancreatic islets of Langerhans: evidence for a paracrine transmitter interplay. J Cell Sci 2004;117:3749–3758. [PubMed: 15252115]

Gasnier B. The SLC32 transporter, a key protein for the synaptic release of inhibitory amino acids. Pflugers Arch Eur J Physiol 2004;447:756–759. [PubMed: 12750892]

Ghosh KK, Haverkamp S, Wässle H. Glutamate receptors in the rod pathway of the mammalian retina. J Neurosci 2001;21:8636–8647. [PubMed: 11606651]

Glykys J, Mody I. Activation of $GABA_A$ receptors: views from outside the synaptic cleft. Neuron 2007;56:763–770. [PubMed: 18054854]

Grünert U, Wässle H. GABA-like immunoreactivity in the macaque monkey retina: a light and electron microscopic study. J Comp Neurol 1990;297:509–524. [PubMed: 2384611]

Guastella J, Nelson N, Nelson H, Czyzyk L, Keynan S, Miedel MC, Davidson N, Lester HA, Kanner BI. Cloning and expression of a rat brain GABA transporter. Science 1990;249:1303–1306. [PubMed: 1975955]

Haverkamp S, Wässle H. Immunocytochemical analysis of the mouse retina. J Comp Neurol 2000;424:1–23. [PubMed: 10888735]

Haverkamp S, Grünert U, Wässle H. The cone pedicle, a complex synapse in the retina. Neuron 2000;27:85–95. [PubMed: 10939333]

Haverkamp S, Ghosh KK, Hirano AA, Wässle H. Immunocytochemical description of five bipolar cell types of the mouse retina. J Comp Neurol 2003;455:463–476. [PubMed: 12508320]

Hirano AA, Brandstätter JH, Brecha NC. Cellular distribution and subcellular localization of molecular components of vesicular transmitter release in horizontal cells of rabbit retina. J Comp Neurol 2005;488:70–81. [PubMed: 15912504]

Hirano AA, Brandstätter JH, Vila A, Brecha NC. Robust syntaxin-4 immunoreactivity in mammalian horizontal cell processes. Vis Neurosci 2007;24:489–502. [PubMed: 17640443]

Honda S, Yamamoto M, Saito N. Immunocytochemical localization of three subtypes of GABA transporter in rat retina. Brain Res Mol Brain Res 1995;33:319–325. [PubMed: 8750892]

Hu J, Quick MW. Substrate-mediated regulation of gamma-aminobutyric acid transporter 1 in rat brain. Neuropharmacology 2008;54:309–318. [PubMed: 17991494]

Hu M, Bruun A, Ehinger B. Expression of GABA transporter subtypes (GAT1, GAT3) in the adult rabbit retina. Acta Ophthalmol Scand 1999;77:255–260. [PubMed: 10406141]

Huang B, Mitchell CK, Redburn-Johnson DA. GABA and $GABA_A$ receptor antagonists alter developing cone photoreceptor development in neonatal rabbit retina. Vis Neurosci 2000;17:925–935. [PubMed: 11193109]

Hull C, Li GL, von Gersdorff H. GABA transporters regulate a standing $GABA_C$ receptor-mediated current at a retinal presynaptic terminal. J Neurosci 2006;26:6979–6984. [PubMed: 16807327]

Ichinose T, Lukasiewicz PD. GABA transporters regulate inhibition in the retina by limiting $GABA_C$ receptor activation. J Neurosci 2002;22:3285–3292. [PubMed: 11943830]

Ikegaki N, Saito N, Hashima M, Tanaka C. Production of specific antibodies against GABA transporter subtypes (GAT1, GAT2, GAT3) and their application to immunocytochemistry. Brain Res Mol Brain Res 1994;26:47–54. [PubMed: 7854065]

Isaacson JS, Solis JM, Nicoll RA. Local and diffuse synaptic actions of GABA in the hippocampus. Neuron 1993;10:165–175. [PubMed: 7679913]

Jellali A, Stussi-Garaud C, Gasnier B, Rendon A, Sahel J-A, Dreyfus H, Picaud S. Cellular localization of the vesicular inhibitory amino acid transporter in the mouse and human retina. J Comp Neurol 2002;449:76–87. [PubMed: 12115694]

Johnson J, Chen TK, Rickman DW, Evans C, Brecha NC. Multiple γ-aminobutyric acid plasma membrane transporters (GAT-1, GAT-2, GAT-3) in the rat retina. J Comp Neurol 1996;375:212–224. [PubMed: 8915826]

Johnson J, Tian N, Caywood MS, Reimer RJ, Edwards RH, Copenhagen DR. Vesicular neurotransmitter transporter expression in developing postnatal rodent retina: GABA and glycine precede glutamate. J Neurosci 2003;23:518–529. [PubMed: 12533612]

Kanner BI. Structure and function of sodium-coupled GABA and glutamate transporters. J Membrane Biol 2006;213:89–100. [PubMed: 17417704]

Kao YH, Lassova L, Bar-Yehuda T, Edwards RH, Sterling P, Vardi N. Evidence that certain retinal bipolar cells use both glutamate and GABA. J Comp Neurol 2004;478:207–218. [PubMed: 15368537]

Keros S, Hablitz JJ. Subtype-specific GABA transporter antagonists synergistically modulate phasic and tonic $GABA_A$ conductances in rat neocortex. J Neurophysiol 2005;94:2073–2085. [PubMed: 15987761]

Liu QR, López-Corcuera B, Mandiyan S, Nelson H, Nelson N. Molecular characterization of four pharmacologically distinct gamma-aminobutyric acid transporters in mouse brain [corrected]. J Biol Chem 1993;268:2106–2112. [PubMed: 8420981]

Liu Y, Edwards RH. The role of vesicular transport proteins in synaptic transmission and neural degeneration. Annu Rev Neurosci 1997;20:125–156. [PubMed: 9056710]

Lu CC, Hilgemann DW. GAT1 ($GABA:Na^+:Cl^-$) cotransport function. Steady state studies in giant *Xenopus* oocyte membrane patches. J Gen Physiol 1999;114:429–444. [PubMed: 10469733]

McIntire SL, Reimer RJ, Schuske K, Edwards RH, Jorgensen EM. Identification and characterization of the vesicular GABA transporter. Nature 1997;389:870–876. [PubMed: 9349821]

Messersmith EK, Redburn DA. Kainic acid lesioning alters development of the outer plexiform layer in neonatal rabbit retina. Int J Dev Neurosci 1990;8:447–461. [PubMed: 2251935]

Messersmith EK, Redburn DA. Gamma-aminobutyric acid immunoreactivity in multiple cell types of the developing rabbit retina. Vis Neurosci 1992;8:201–211. [PubMed: 1547159]

Messersmith EK, Redburn DA. The role of GABA during development of the outer retina in the rabbit. Neurochem Res 1993;18:463–470. [PubMed: 8474569]

Minelli A, Brecha NC, Karschin C, DeBiasi S, Conti F. GAT-1, a high-affinity GABA plasma membrane transporter, is localized to neurons and astroglia in the cerebral cortex. J Neurosci 1995;15:7734–7746. [PubMed: 7472524]

Minelli A, DeBiasi S, Brecha NC, Zuccarello LV, Conti F. GAT-3, a high-affinity GABA plasma membrane transporter, is localized to astrocytic processes, and it is not confined to the vicinity of GABAergic synapses in the cerebral cortex. J Neurosci 1996;16:6255–6264. [PubMed: 8815906]

Morrow EM, Chen CM, Cepko CL. Temporal order of bipolar cell genesis in the neural retina. Neural Dev 2008;3:2. [PubMed: 18215319]

Nelson N. The family of Na^+/Cl^- neurotransmitter transporters. J Neurochem 1998;71:1785–1803. [PubMed: 9798903]

Nickerson PE, Emsley JG, Myers T, Clarke DB. Proliferation and expression of progenitor and mature retinal phenotypes in the adult mammalian ciliary body after retinal ganglion cell injury. Invest Ophthalmol Vis Sci 2007;48:5266–5275. [PubMed: 17962482]

O'Malley DM, Sandell JH, Masland RH. Co-release of acetylcholine and GABA by the starburst amacrine cells. J Neurosci 1992;12:1394–1408. [PubMed: 1556600]

Olney JW. An electron microscopic study of synapse formation, receptor outer segment development, and other aspects of developing mouse retina. Invest Ophthalmol Vis Sci 1968;7:250–268.

Osborne NN, Patel S, Beaton DW, Neuhoff V. GABA neurones in retinas of different species and their postnatal development in situ and in culture in the rabbit retina. Cell Tissue Res 1986;243:117–123. [PubMed: 3510739]

Owens DF, Kriegstein AR. Is there more to GABA than synaptic inhibition? Nat Rev Neurosci 2002;3:715–727. [PubMed: 12209120]

Peichl L, González-Soriano J. Morphological types of horizontal cell in rodent retinae: a comparison of rat, mouse, gerbil, and guinea pig. Vis Neurosci 1994;11:501–517. [PubMed: 8038125]

Pourcho RG. Autoradiographic localization of [^{3}H]muscimol in the cat retina. Brain Res 1981;215:187–199. [PubMed: 7260587]

Pourcho RG, Owczarzak MT. Distribution of GABA immunoreactivity in the cat retina: a light- and electron-microscopic study. Vis Neurosci 1989;2:425–435. [PubMed: 2487080]

Pow DV, Sullivan RK, Williams SM, Scott HL, Dodd PR, Finkelstein D. Differential expression of the GABA transporters GAT-1 and GAT-3 in brains of rats, cats, monkeys and humans. Cell Tissue Res 2005;320:379–392. [PubMed: 15821932]

Quick MW. The role of SNARE proteins in trafficking and function of neurotransmitter transporters. Hdbk Exp Pharmacol 2006;175:181–196.

Rapaport DH, Rakic P, LaVail MM. Spatiotemporal gradients of cell genesis in the primate retina. Perspect Dev Neurobiol 1996;3:147–159. [PubMed: 8931090]

Raven MA, Reese BE. Horizontal cell density and mosaic regularity in pigmented and albino mouse retina. J Comp Neurol 2002;454:168–176. [PubMed: 12412141]

Redburn-Johnson D. GABA as a developmental neurotransmitter in the outer plexiform layer of the vertebrate retina. Perspect Dev Neurobiol 1998;5:261–267. [PubMed: 9777641]

Represa A, Ben-Ari Y. Trophic actions of GABA on neuronal development. Trends Neurosci 2005;28:278–283. [PubMed: 15927682]

Ribak CE, Tong WM, Brecha NC. GABA plasma membrane transporters, GAT-1 and GAT-3, display different distributions in the rat hippocampus. J Comp Neurol 1996;367:595–606. [PubMed: 8731228]

Rich KA, Zhan Y, Blanks JC. Migration and synaptogenesis of cone photoreceptors in the developing mouse retina. J Comp Neurol 1997;388:47–63. [PubMed: 9364238]

Richerson GB, Wu Y. Dynamic equilibrium of neurotransmitter transporters: not just for reuptake anymore. J Neurophysiol 2003;90:1363–1374. [PubMed: 12966170]

Rowan S, Cepko CL. Genetic analysis of the homeodomain transcription factor Chx10 in the retina using a novel multifunctional BAC transgenic mouse reporter. Dev Biol 2004;271:388–402. [PubMed: 15223342]

Sagné C, El Mestikawy S, Isambert MF, Hamon M, Henry JP, Giros B, Gasnier B. Cloning of a functional vesicular GABA and glycine transporter by screening of genome databases. FEBS Lett 1997;417:177–183. [PubMed: 9395291]

Schnitzer J, Rusoff AC. Horizontal cells of the mouse retina contain glutamic acid decarboxylase-like immunoreactivity during early developmental stages. J Neurosci 1984;4:2948–2955. [PubMed: 6502214]

Schwartz EA. Depolarization without calcium can release gamma-aminobutyric acid from a retinal neuron. Science 1987;238:350–355. [PubMed: 2443977]

Schwartz EA. Transport-mediated synapses in the retina. Physiol Rev 2002;82:875–891. [PubMed: 12270946]

Spoerri PE. Neurotrophic effects of GABA in cultures of embryonic chick brain and retina. Synapse 1988;2:11–22. [PubMed: 3420527]

Südhof TC. The synaptic vesicle cycle. Annu Rev Neurosci 2004;27:509–547. [PubMed: 15217342]

Tafoya LC, Mameli M, Miyashita T, Guzowski JF, Valenzuela CF, Wilson MC. Expression and function of SNAP-25 as a universal SNARE component in GABAergic neurons. J Neurosci 2006;26:7826–7838. [PubMed: 16870728]

Takamori S, Riedel D, Jahn R. Immunoisolation of GABA-specific synaptic vesicles defines a functionally distinct subset of synaptic vesicles. J Neurosci 2000;20:4904–4911. [PubMed: 10864948]

Uesugi R, Yamada M, Mizuguchi M, Baimbridge KG, Kim SU. Calbindin D-28K and parvalbumin immunohistochemistry in developing rat retina. Exp Eye Res 1992;54:491–499. [PubMed: 1623935]

Unsoeld T, Stradomska AM, Wang R, Rathjen FG, Juttner R. Early maturation of GABAergic synapses in mouse retinal ganglion cells. Int J Dev Neurosci 2008;26:233–238. [PubMed: 18207351]

Versaux-Botteri C, Pochet R, Nguyen-Legros J. Immunohistochemical localization of GABA-containing neurons during postnatal development of the rat retina. Invest Ophthalmol Vis Sci 1989;30:652–659. [PubMed: 2649448]

Wang C-T, Blankenship AG, Anishchenko A, Elstrott J, Fikhman M, Nakanishi S, Feller MB. $GABA_A$ receptor-mediated signaling alters the structure of spontaneous activity in the developing retina. J Neurosci 2007;27:9130–9140. [PubMed: 17715349]

Wang D, Quick MW. Trafficking of the plasma membrane gamma-aminobutyric acid transporter GAT1. Size and rates of an acutely recycling pool. J Biol Chem 2005;280:18703–18709. [PubMed: 15778221]

Wässle H, Chun MH. GABA-like immunoreactivity in the cat retina: light microscopy. J Comp Neurol 1989;279:43–54. [PubMed: 2913060]

Weidman TA, Kuwabara T. Postnatal development of the rat retina. An electron microscopic study. Arch Ophthalmol 1968;79:470–484. [PubMed: 5640327]

Wojcik SM, Katsurabayashi S, Guillemin I, Friauf E, Rosenmund C, Brose N, Rhee JS. A shared vesicular carrier allows synaptic corelease of GABA and glycine. Neuron 2006;50:575–587. [PubMed: 16701208]

Wong WT, Wong RO. Changing specificity of neurotransmitter regulation of rapid dendritic remodeling during synaptogenesis. Nature neuroscience 2001;4:351–352.

Wu Y, Wang W, Diez-Sampedro A, Richerson GB. Nonvesicular inhibitory neurotransmission via reversal of the GABA transporter GAT-1. Neuron 2007;56:851–865. [PubMed: 18054861]

Yamasaki EN, Barbosa VD, De Mello FG, Hokoc JN. GABAergic system in the developing mammalian retina: dual sources of GABA at early stages of postnatal development. Int J Dev Neurosci 1999;17:201–213. [PubMed: 10452364]

Yamauchi A, Uchida S, Kwon HM, Preston AS, Robey RB, Garcia-Perez A, Burg MB, Handler JS. Cloning of a Na^+- and Cl^--dependent betaine transporter that is regulated by hypertonicity. J Biol Chem 1992;267:649–652. [PubMed: 1370453]

Young RW. Cell differentiation in the retina of the mouse. Anat Rec 1985;212:199–205. [PubMed: 3842042]

Young S, Rothbard J, Parker PJ. A monoclonal antibody recognising the site of limited proteolysis of protein kinase C. Eur J Biochem 1988;173:247–252. [PubMed: 2451608]

Zheng JJ, Lee S, Zhou ZJ. A developmental switch in the excitability and function of the starburst network in the mammalian retina. Neuron 2004;44:851–864. [PubMed: 15572115]

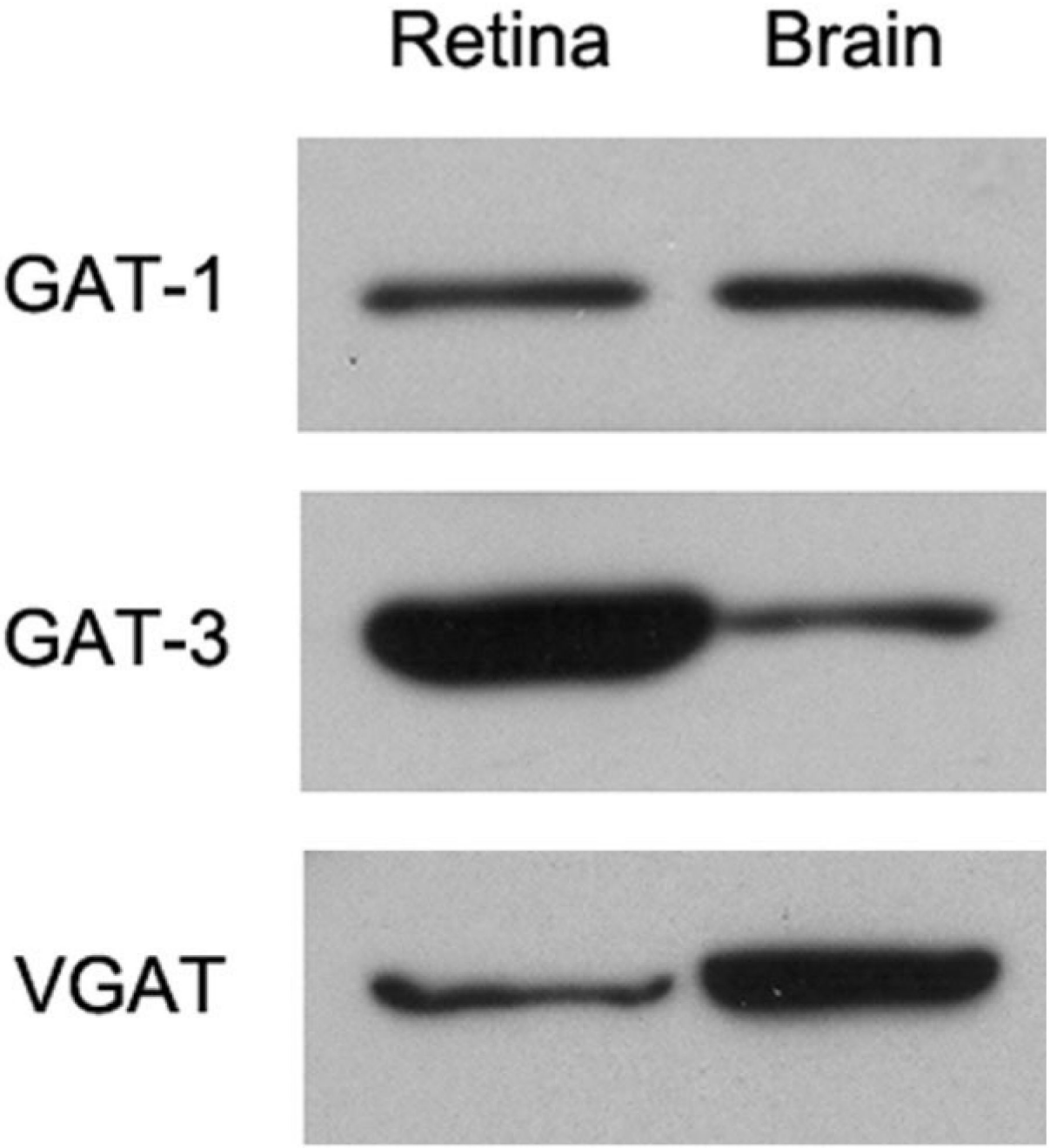

Figure 1.
Immunoblot of GAT-1, GAT-3, and VGAT in adult mouse retina and brain. The affinity-purified GAT-1 (346O; 1:1,000) and GAT-3 (374D; 1:1,000) polyclonal and the VGAT (Synaptic Systems No. 131011; 1:1,500) monoclonal antibodies detected single bands at 67, 71, and 57 kD, respectively. Retina and brain total protein: 8–10 μg per lane for the GAT-1 and VGAT immunoblots, retina total protein 8–10 μg per lane, and brain total protein 20 μg per lane for the GAT-3 immunoblot.

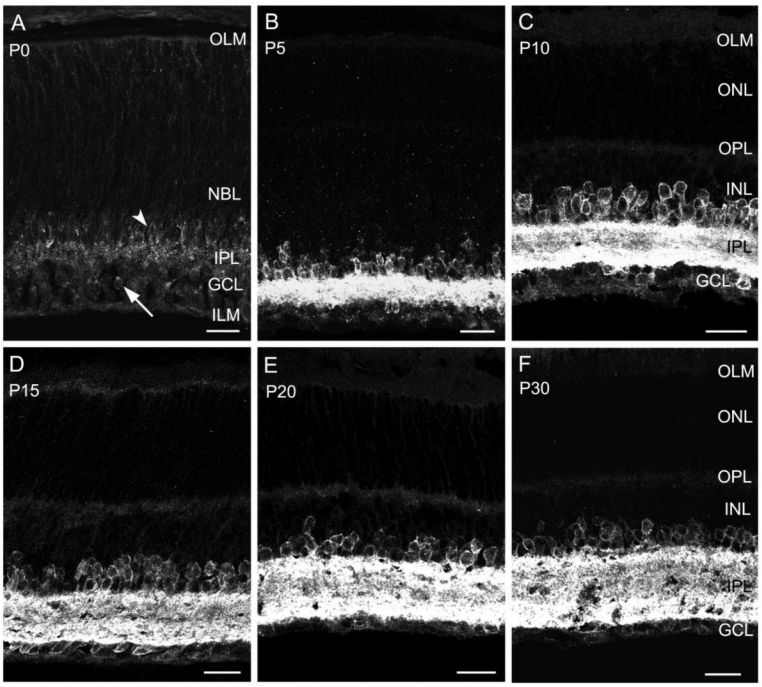

Figure 2.

GAT-1 immunoreactivity in the developing mouse retina. A–F: Vertical sections from P0 (A), P5 (B), P10 (C), P15 (D), P20 (E), and P30 (F) mouse retinas. GAT-1 immunostaining is at or near the plasma membrane of amacrine and displaced amacrine cell somata and in processes and puncta in the IPL from P0 to P30. A: GAT-1 immunoreactivity is weakly expressed in the INL, IPL, and GCL at P0. An amacrine cell body and a displaced amacrine cell body are indicated by an arrowhead and arrow, respectively. D,E: Very weak GAT-1 staining is also seen in Müller cell processes during the second postnatal week; see the OPL and ONL at P15 (D) and P20 (E). For all ages, confocal images were obtained from three to five optical sections with an average total thickness of 3–5 μm and compressed for viewing. NBL, neuroblast layer; OLM, outer limiting membrane; ONL, outer nuclear layer; OPL, outer plexiform layer; ILM, inner limiting membrane; INL, inner nuclear layer; IPL, inner plexiform layer; GCL, ganglion cell layer. Scale bars = 20 μm.

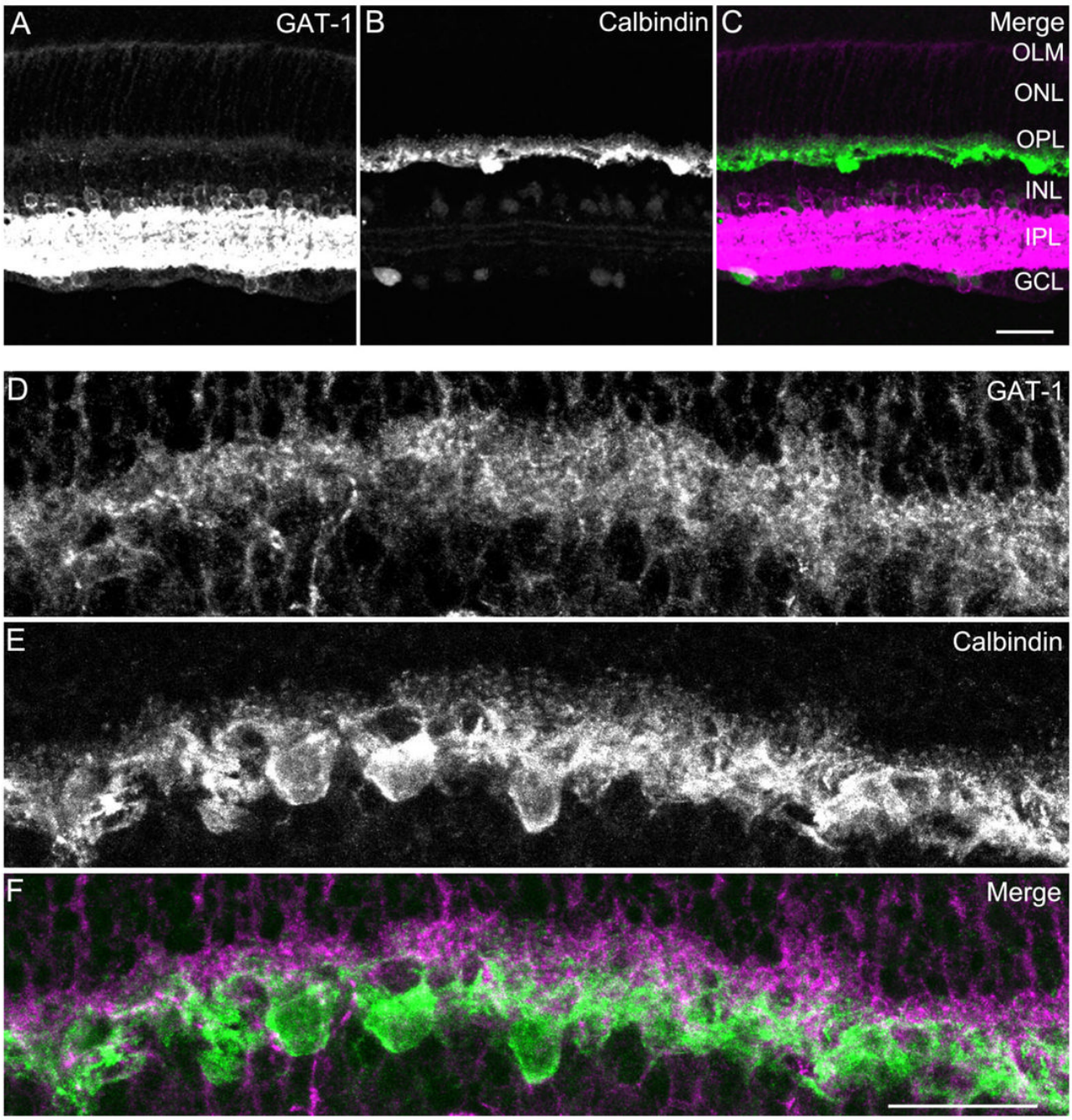

Figure 3.

GAT-1 immunoreactivity is not localized to horizontal cell bodies or processes. A vertical section through a P48 mouse retina doubly labeled with antibodies to GAT-1 and calbindin D-28K (calbindin). **A:** Weak GAT-1 immunostaining is in the OPL; robust GAT-1 immunostaining is in amacrine cell somata and processes in the inner retina. **B:** Calbindin is expressed by horizontal cell somata and processes in the outer retina and some amacrine and ganglion cell somata and their processes in the inner retina. **C:** Merged image showing the localization of GAT-1 (magenta) and calbindin (green) immunoreactivity in the retina. **D–F:** Enlarged images showing the distribution of calbindin and GAT-1 immunoreactivities in the OPL. D: GAT-1 immunoreactivity in cellular processes in the OPL. E: Calbindin

immunoreactivity in horizontal cell somata and their processes. F: Merged image. GAT-1-immunoreactive processes surround calbindin-immunoreactive horizontal cell tips. Confocal images were obtained from five to eight optical sections with an average total thickness of 5–8 μ m and compressed for viewing. Scale bars = 20 μ m in C (applies to A-C); 20 μ m in F (applies to D-F).

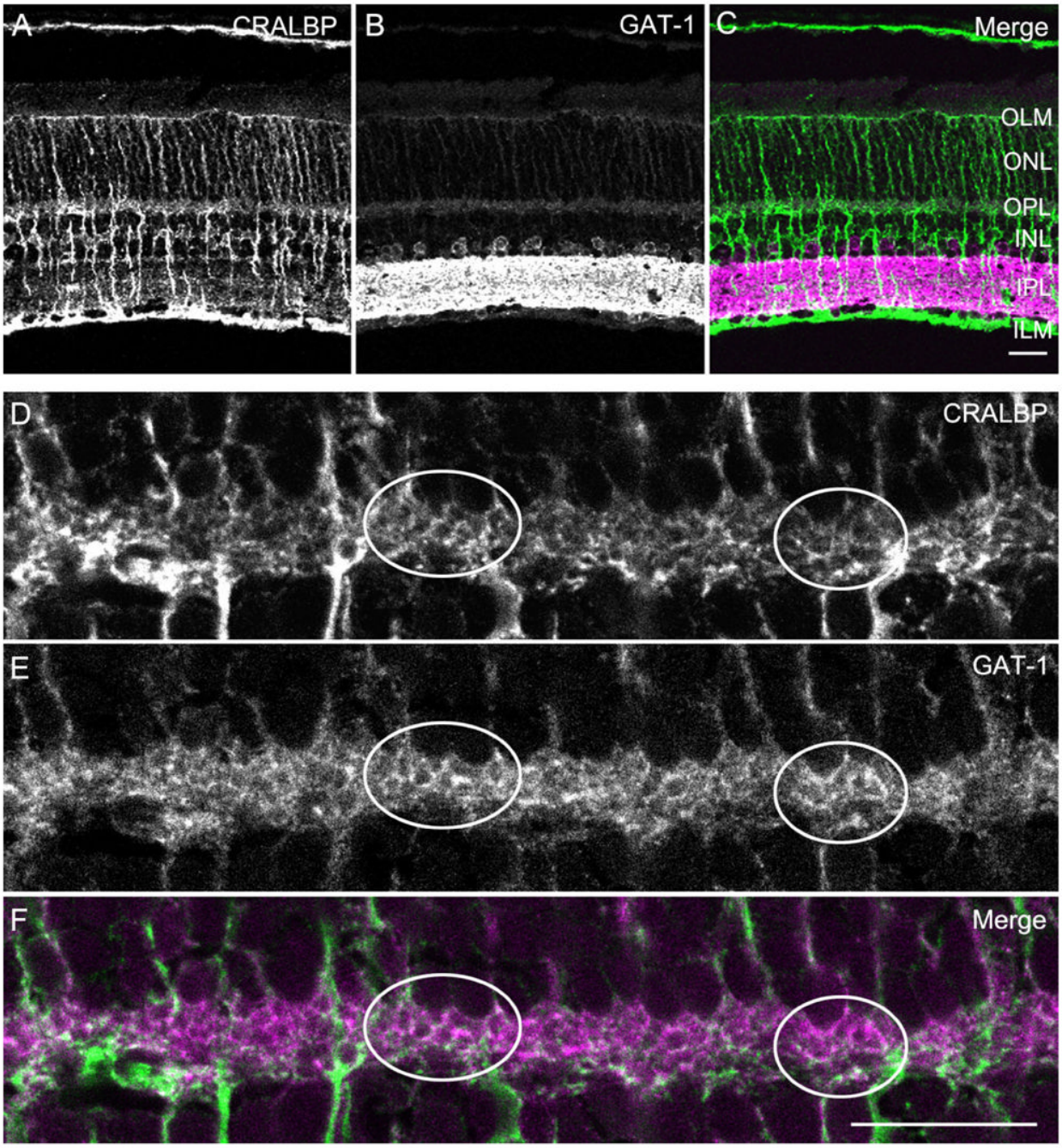

Figure 4.

CRALBP and GAT-1 immunoreactivities are coexpressed in Müller cell processes. A vertical section through a P48 mouse retina that was doubly immunostained with antibodies to CRALBP and GAT-1. **A:** CRALBP-immunostained Müller cell somata and their processes in all layers of the retina. **B:** Weak GAT-1 immunoreactivity is present in the outer retina; strong GAT-1 immunoreactivity is distributed to amacrine cell and displaced amacrine cell somata and their processes in the IPL. **C:** Merged image showing the colocalization of CRALBP (green) and GAT-1 (magenta) immunoreactivities. **D–F:** Enlarged images showing the distribution of CRALBP and GAT-1 immunoreactivity in the OPL. D: CRALBP-immunoreactive processes in the OPL. E: GAT-1-immunoreactive processes in the OPL. F:

Merged image showing the coexpression of CRALBP and GAT-1 immunoreactivity in the OPL, indicating that GAT-1 immunoreactivity is localized to Müller cell processes. Ovals illustrate examples of CRALBP-immunostained processes with GAT-1 immunoreactivity. Confocal images were obtained from five to eight optical sections with an average total thickness of 5– 8 μ m and compressed for viewing. Scale bars = 20 μ m in C (applies to A-C); 20 μ m in F (applies to D–F).

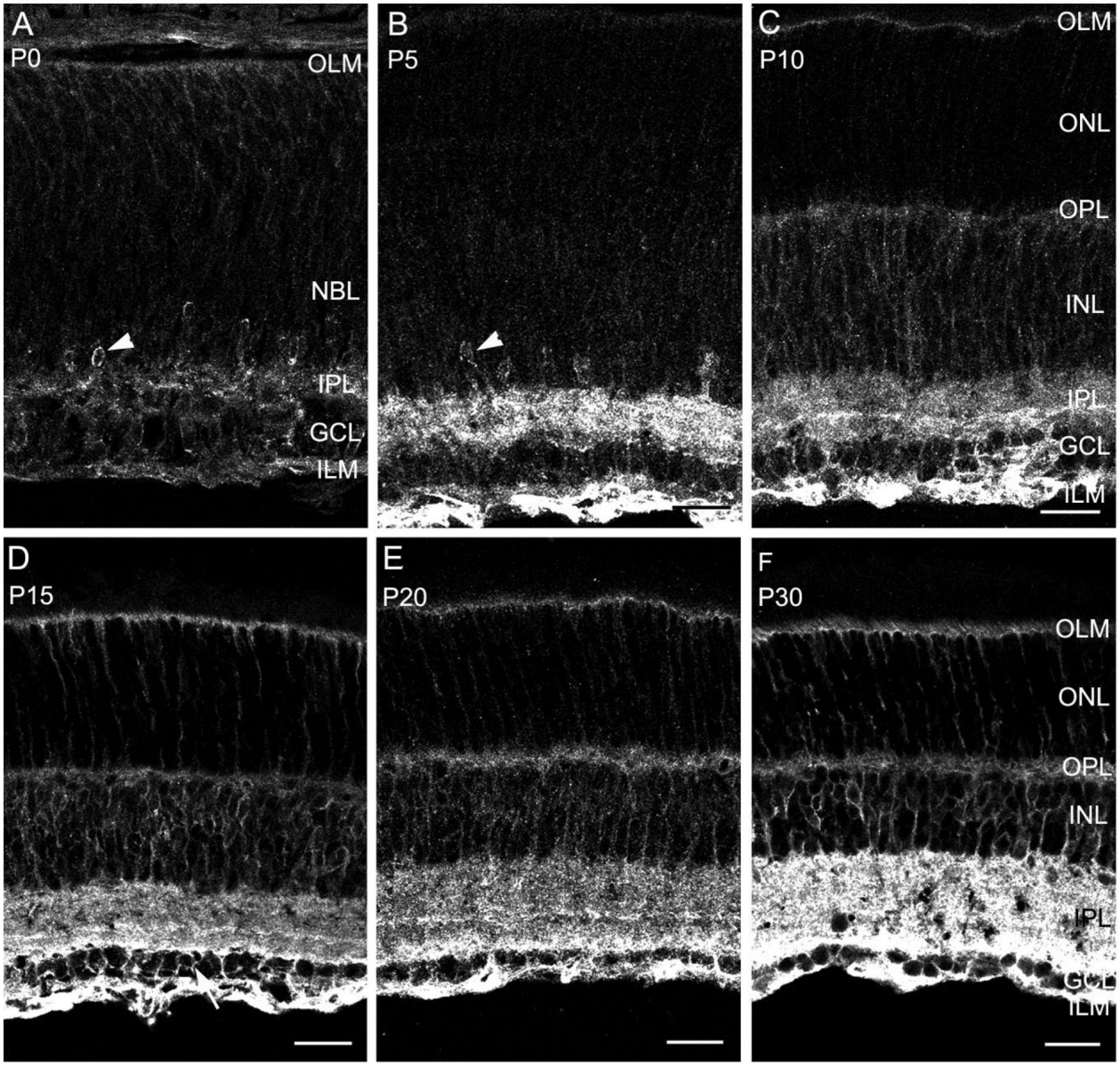

Figure 5.

GAT-3 immunoreactivity in the developing mouse retina. **A–F:** Vertical sections from P0 (A), P5 (B), P10 (C), P15 (D), P20 (E), and P30 (F) mouse retinas. A,B: GAT-3 immunostaining is more prominent in the inner retina during the first postnatal week. An amacrine cell body is indicated by an arrowhead. C–F: GAT-3 immunoreactivity is expressed predominantly by Müller cells and their processes that are distributed from the OLM to the ILM. GAT-3 immunoreactivity reaches the adult pattern during the second postnatal week and shows the adult level of staining intensity at P30. Confocal images were obtained from three to five optical sections with an average total thickness of 3–5 μ m and compressed for viewing. Scale bars = 20 μ m.

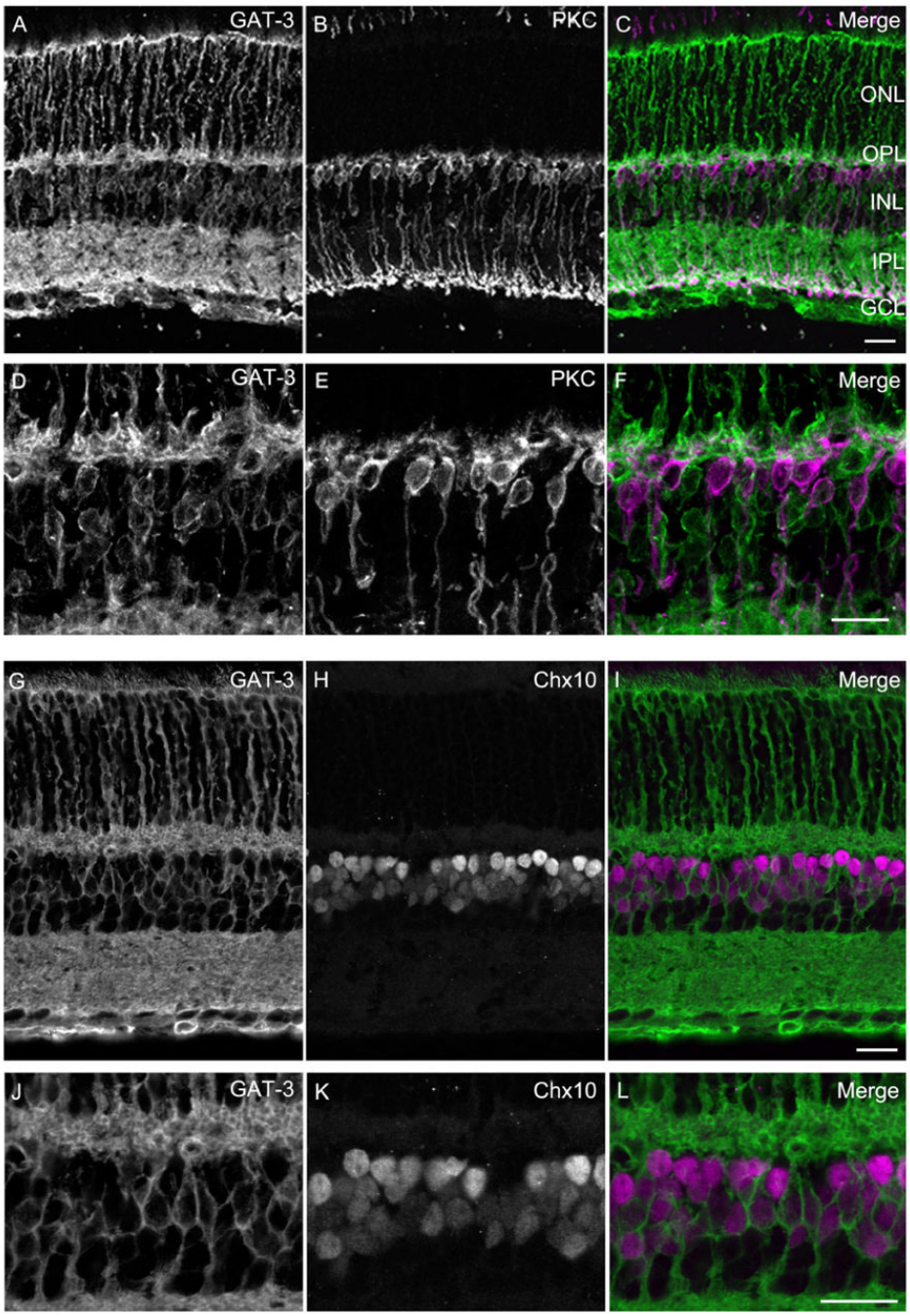

Figure 6.

GAT-3 and PKC, and GAT-3 and Chx10 double labeling showing that GAT-3-immunoreactive processes ensheath bipolar cell somata. Images are of two vertical sections through an adult retina doubly immunostained with antibodies to GAT-3 and PKC and to GAT-3 and Chx10, respectively. **A,G:** GAT-3 immunoreactivity expressed by Müller cell somata and processes in the INL and their processes in the OPL. GAT-3 immunoreactivity is also expressed by amacrine cell bodies and their processes in the IPL. **B:** PKC immunoreactivity is in rod bipolar cell bodies in the INL as well as their axons in the IPL and their dendrites in the OPL. **C:** Merged image showing the localization of GAT-3 (green) and PKC (magenta) immunoreactivity in the retina. **D–F:** Enlarged images of GAT-3 (D) and PKC (E) double

labeling, showing that bipolar cell somata are ensheathed by Müller cell processes in the INL (F). GAT-3 (**G**) and Chx10 (**H**) immunoreactivity distributed to the nuclei of rod and cone bipolar cells and some Müller cell somata in the INL (Rowan and Cepko, 2004). **I:** Merged image showing the localization of GAT-3 and Chx10 immunoreactivity in the retina. **J–L:** Enlarged images of GAT-3 (J) and Chx10 (K) double labeling showing that the bipolar cell somata are ensheathed by Müller cell processes in the INL (L). Some of the Müller cell nuclei also show immunoreactivity of Chx10. Confocal images were obtained from five (A–F) or three (G–L) optical sections with an average total thickness of 5μ m (A–F) and 0.6 μ m (G–L) and compressed for viewing. Scale bars = 20 μ m in C (applies to A–C); 20 μ m in F (applies to D–F); 20 μ m in I (applies to G–I); 20 μ m in L (applies to J–L).

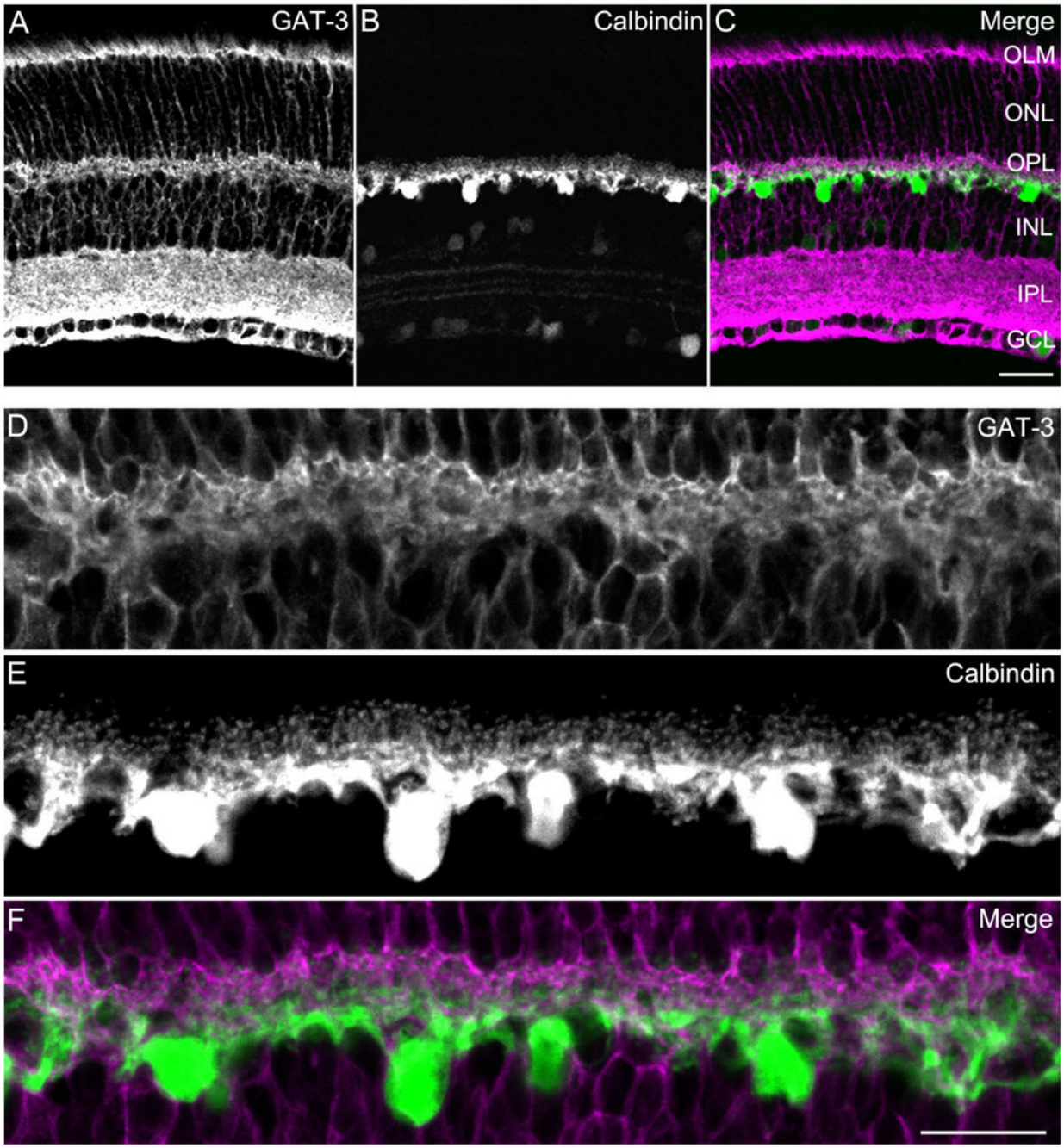

Figure 7.

GAT-3 and calbindin immunostaining showing that GAT-3 immunoreactivity is distributed to Müller cell processes in the outer retina. Images are of a vertical section through a P48 mouse retina doubly immunostained with antibodies to GAT-3 and calbindin. **A:** GAT-3 immunostaining in amacrine and Müller cells and their processes. **B:** Calbindin immunostaining in horizontal cells, amacrine cells, and displaced amacrine cells and their processes. **C:** Merged image showing the localization of GAT-3 (magenta) and calbindin (green) immunoreactivities in the retina. **D–F:** Enlarged images showing GAT-3 and GAT-3 double staining in the OPL. D: GAT-3-immunoreactive processes in the OPL. E: Calbindin immunoreactivity in horizontal cells and their processes. F: Merged image showing GAT-3

immunostaining in the OPL surrounding the tips of horizontal cell processes. Confocal images were obtained from five to eight optical sections with an average total thickness of 5– 8 μ m and compressed for viewing. Scale bars = 20 μ m in C (applies to A–C); 20 μ m in F (applies to D–F).

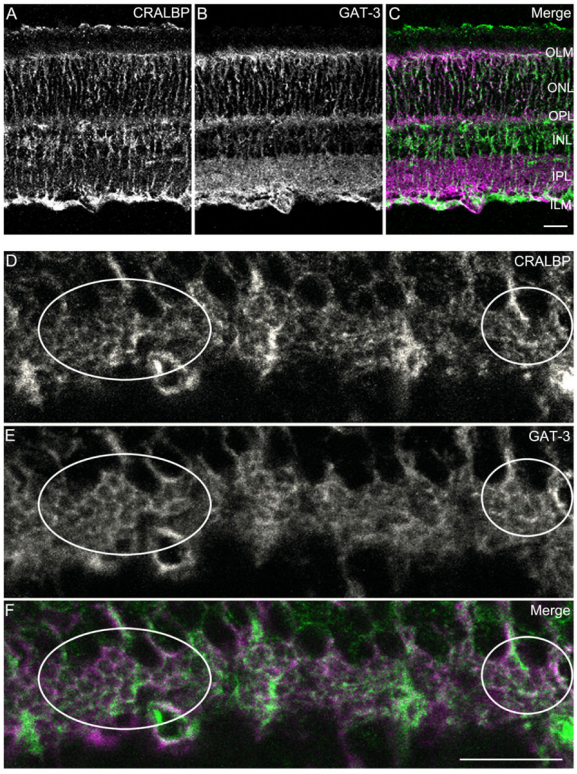

Figure 8.

CRALBP and GAT-3 immunostaining in the retina showing that GAT-1 immunoreactivity is also distributed to Müller cell processes. Images of a vertical section through a P48 mouse retina doubly immunostained with antibodies to CRALBP and GAT-3. **A:** CRALBP immunostaining is in Müller cell processes extending from the OLM to the ILM. **B:** GAT-3 immunostaining in the Müller cells and their processes and in some amacrine cells and their processes in the IPL. **C:** Merged image showing the localization of CRALBP (green) and GAT-3 (magenta) immunostaining in the retina. **D-F:** Enlarged images showing the distribution of CRALBP and GAT-3 immunoreactivities in the OPL. D: CRALBP immunostained processes in the OPL. E: GAT-3-immunoreactive processes in the OPL. F: Merged image showing the colocalization of CRALBP and GAT-3 in Müller cell processes in the OPL. Ovals illustrate examples of the colocalization of CRALBP and GAT-3 immunoreactivity in the OPL. Confocal images were obtained from five to eight optical sections with an average total thickness of 5– 8 μ m and compressed for viewing. Scale bars = 20 μ m in C (applies to A–C); 20 μ m in F (applies to D-F).

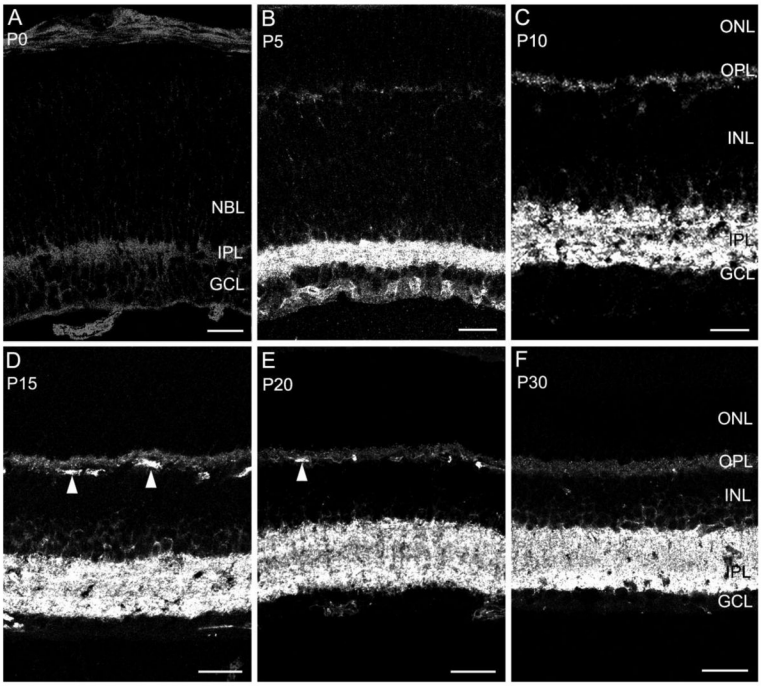

Figure 9.

VGAT immunostaining in the developing mouse retina. **A–F:** Vertical sections from P0 (A), P5 (B), P10 (C), P15 (D), P20 (E), and P30 (F) mouse retinas. VGAT immunoreactivity is observed in amacrine and displaced amacrine cell somata as well as in processes in the IPL at P5 to P30. A: Weak VGAT immunoreactivity is seen in horizontal cell processes in the OPL at P5. Arrow indicates an amacine cell body. C–E: Robust VGAT immunostaining is observed beginning at P5 (B). Some blood vessels near the OPL are labeled as seen in D and E (arrowheads); this is due to nonspecific staining associated with the VGAT monoclonal antibody (Synaptic Systems, Göttingen, Germany; No. 131 011). Nonspecific staining of blood vessels is due to nonspecific labeling of the secondary antibody. Scale bars = 20 μ m.

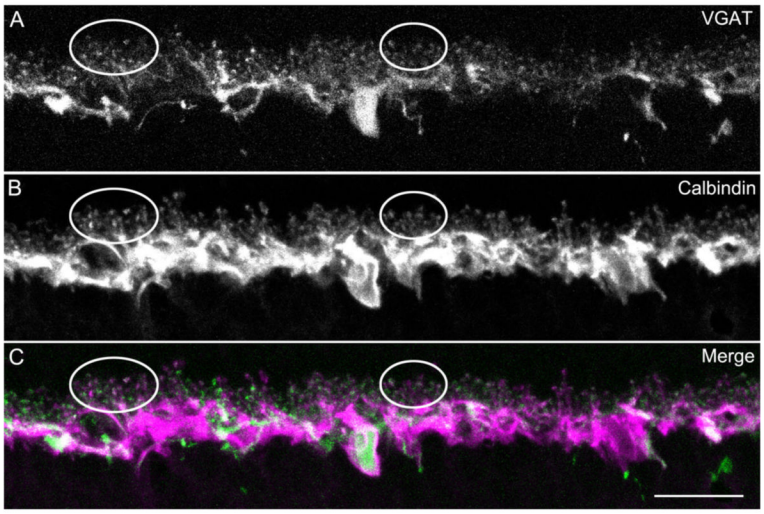

Figure 10.

VGAT and calbindin immunostaining in the OPL of adult mouse retina. **A:** VGAT immunoreactivity is distributed to horizontal cells and their processes. **B:** Calbindin immunoreactivity is also distributed to horizontal cells and their processes. **C:** Merged image showing the colocalization of VGAT (green) and calbindin (magenta) immunoreactivities. Ovals highlight examples of colocalization of VGAT and calbindin immunoreactivity in horizontal cell tips in the OPL. Confocal images were obtained from five optical sections with an average total thickness of 5 μ m and compressed for viewing. Scale bar = 20 μ m.

TABLE 1

Antibodies Used in This Study[1]

Antibody	Host	Antigen	Source	Catalog No.	Dilution	References
Western blotting						
GAT-1[2]	Rb	C-terminus of rat GAT-1 (aa 588-599) coupled to keyhole limpet hemocyanin (KLH)	UCLA/Brecha	346O	1:1,000	This report, Figure 1
GAT-3[3]	Rb	C-terminus of rat GAT-3 (aa 607-627) coupled to KLH	UCLA/Brecha	374D	1:1,000	This report, Figure 1
VGAT	Ms	N-terminus of rat VGAT (aa 75-87) coupled to KLH	Synaptic Systems, Göttingen, Germany	131 011	1:1,500	This report, Figure 1
Immunohistochemistry						
GAT-1[2]	Rb	C-terminus of rat GAT-1 (aa 588-599) coupled to KLH	UCLA/Brecha	346O	1:500	Johnson et al., 1996
GAT-3[3]	Rb	C-terminus of rat GAT-3 (aa 607-627) coupled to KLH	UCLA/Brecha	374D	1:500	Johnson et al., 1996
VGAT	Ms	N-terminus of rat VGAT (aa 75-87) coupled to KLH	Synaptic Systems, Göttingen, Germany	131 011	1:1,000	Tafoya et al., 2006; Baer et al., 2007
VGAT-N2	Rb	Predicted 99 amino acids of the rat VGAT N-terminus fused to glutathione S-transferase	Dr. Richard J. Reimer; Stanford University School of Medicine, CA	N/A	1:1,000	Chaudhry et al., 1998; Cueva et al., 2002
Calbindin	Ms	Bovine kidney calbindin D-28K	Sigma-Aldrich, Inc., St. Louis, MO	C9848	1:2,500	Haverkamp and Wässle, 2000
Calbindin	Rb	Recombinant rat calbindin D-28K	Swant, Bellinzona, Switzerland	CB38	1:8,000	Garcia-Segura et al., 1984; Dassesse et al., 1998
CRALBP	Ms	Recombinant full-length human CRALBP	Abcam Inc., Cambridge, MA	ab15051	1:1,000	Bunt-Milam and Saari, 1983
PKC	Ms	Hinge region of the calcium-activated, phospholipid-dependent protein kinase C from bovine brain; clone MC5	Biodesign International, Saco, ME	K01107M	1:200	Young et al., 1988; Ghosh et al., 2001
Chx10	Shp	Recombinant human Chx10 protein, N-terminus	Millipore Corporation., Temecula, CA	AB9016	1:2,500	Dorval et al., 2006; Nickerson et al., 2007

[1] Antibody type: Rb, rabbit polyclonal; Ms, mouse monoclonal; Shp, sheep polyclonal. Information supplied by the vendor unless otherwise shown.

[2] GAT-1 AB1570; Millipore (Temecula, CA).

[3] GAT-3 AB1574; Millipore (Temecula, CA).